

A Novel Robust Optimization Model for Nonlinear Support Vector Machine

Francesca Maggioni^{a,*}, Andrea Spinelli^a

^a*Department of Management, Information and Production Engineering, University of Bergamo, Viale G. Marconi 5, Dalmine 24044, Italy*

Abstract

In this paper, we present new optimization models for Support Vector Machine (SVM), with the aim of separating data points in two or more classes. The classification task is performed by means of nonlinear classifiers induced by kernel functions. Along with a deterministic formulation in which data are assumed to be perfectly known, we propose a robust extension with bounded-by-norm uncertainty sets. Robust optimization techniques allow to protect the models against uncertainties arising during the collection of real-world observations. Closed-form expressions for the bounds of the uncertainty sets in the feature space for typically used kernel functions have been derived. Extensive numerical results on real-world datasets show the benefits of the proposed classifiers in comparison with various alternatives in the SVM literature.

Keywords: Machine Learning, Nonlinear Support Vector Machine, Robust Optimization

1. Introduction

Support Vector Machine (SVM) is one of the main supervised *Machine Learning* (ML) techniques commonly deployed for classification and regression purposes. Within the *Operational Research* (OR) domain, supervised ML methods are designed to support better decision-making and solve hard optimization problems (Gambella et al. (2021)). To this end, a plethora of methodologies have been devised and applied to various OR fields (De Bock et al. (2023)). In particular, combinatorial optimization (Bengio et al. (2021); Wei et al. (2023)), customer churn prediction (Chen et al. (2012); Maldonado et al. (2020); Szlag & Słowiński (2023)), banking (Yao et al. (2017); Doumpos et al. (2023)) and maritime industry (Mi et al. (2019); Raesi et al. (2023)).

Currently, deep learning algorithms are adopted whenever classical ML methods fail to capture complex relationships between input data both for classification and regression tasks (Gambella et al. (2021)). Nevertheless, the advantage of mathematical programming approaches to model deep neural networks has been explored only for small-sized datasets, and without a guarantee on the effectiveness of the performance (Gunnarsson et al. (2021)). For this reason, the investigation of novel ML techniques is a relevant ongoing research issue (Maldonado et al. (2022)).

Introduced in Vapnik & Chervonenkis (1974), SVM has outperformed most other ML systems, due to its simplicity and better performances. Therefore, it has been applied in many practical

*Corresponding author

Email address: francesca.maggioni@unibg.it (Francesca Maggioni)

research fields, such as finance (Tay & Cao (2001); Luo et al. (2020)), chemistry (Li et al. (2009); Marcelli & De Leone (2020)), medicine (Wang et al. (2018a); Maggioni et al. (2023)), and vehicles smog rating classification (De Leone et al. (2024); Maggioni & Spinelli (2024)), to name a few.

Hard Margin-SVM (HM-SVM) is the original approach formulated in Vapnik & Chervonenkis (1974), consisting in finding a hyperplane classifying observations into two classes, such that the margin, i.e. the ℓ_2 -distance from the hyperplane to the nearest point of each class, is maximized. The underlying hypothesis of the HM-SVM is that training data can always be linearly separated, such that no observation is misclassified. To overcome the assumption of linear separability, in Cortes & Vapnik (1995) the *Soft Margin-SVM* (SM-SVM) is proposed. In this case, the optimal hyperplane seeks a trade-off between the maximization of the margin and the minimization of the training error of misclassification.

In order to improve the accuracy of the method, several SVM variants have been devised in the literature. Specifically, in this paper we focus our attention on the one presented in Liu & Potra (2009). The advantages of this technique over other SVM approaches are mainly due to a two-step procedure. Indeed, rather than considering a single hyperplane, data are firstly separated by means of two parallel hyperplanes as solutions of a SM-SVM model. The final optimal hyperplane is then searched in the strip between them, such that the total number of misclassified points is minimized. Compared to classical SM-SVM, numerical experiments show that this formulation achieves higher levels of computational accuracy.

Nevertheless, training observations may not be always separable by means of hyperplanes and, even with *ad hoc* variants of linear SVM, the misclassification error may be significant. In Boser et al. (1992), the extension of the linear HM-SVM model is introduced, by considering nonlinear transformation of the data. According to this technique, kernel functions are used to embed data points onto a higher-dimensional space (the so-called *feature space*), without increasing the computational complexity of the problem. Several variants of this methodology have been proposed in the ML literature (see for example Bennett & Mangasarian (1992); Mangasarian (1998); Schölkopf et al. (2000); Yajima (2005); Jayadeva et al. (2007); Hao (2010); Peng (2011); Ding & Hua (2014); Ding et al. (2019); Blanco et al. (2020); Cervantes et al. (2020); Du et al. (2021); Jiménez-Cordero et al. (2021)).

For the methods mentioned above, all data points are implicitly assumed to be known exactly. However, in real-world observations this condition may not be always true. Indeed, measurement errors during data collection, random perturbations, presence of noise and other forms of uncertainty may corrupt the quality of input values, resulting in worsening performances of the classification process. In recent years, different techniques have been investigated with the aim of facing uncertainty in ML methods. Among them, *Robust Optimization* (RO) is recognized as one of the main paradigms to protect optimization models against uncertainty (see for example Ben-Tal et al. (2009); Xu et al. (2009); Bertsimas et al. (2011)). RO assumes that all possible realizations of the uncertain parameter belong to a prescribed uncertainty set. The corresponding robust model is then derived by optimizing against the worst-case realization of the parameter across the entire uncertainty set (Bertsimas et al. (2019)). The application of RO strategies typically results in higher predictiveness (Maldonado et al. (2020); Faccini et al. (2022)). For this reason, it is worth designing novel RO models with the aim of improving the accuracy of the

classification process.

In this paper, we present novel SVM models aiming at separating classes of data points. The formulation extends the approach of Liu & Potra (2009) to the context of multiclass and nonlinear classification. In order to protect the model against perturbations, we introduce bounded-by-norm uncertainty sets around each observation and derive the robust counterpart of the deterministic formulation. In addition, our proposal represents a valid contribution to the state of the art on SVM thanks to the computation of the uncertainty set bounds in the feature space as function of the bounds in the input space. This is a novel development in the ML domain.

The main contributions of the paper are four-fold and can be summarized as follows:

- To extend the binary linear SVM approach of Liu & Potra (2009) to the case of multiclass nonlinear classification;
- To formulate a robust SVM model with bounded-by- ℓ_p -norm uncertainty sets with nonlinear classifiers;
- To derive bounds on the radii of the uncertainty sets in the feature space for some of the most used kernel functions in the ML literature;
- To provide extensive numerical experiments based on real-world datasets with the aim of evaluating the performances of the proposed models and comparing the results with the extant methods in the literature.

The remainder of the paper is organized as follows. Section 2 reviews the existing literature on the problem. In Section 3, the notation is introduced, along with a brief discussion on related SVM-type problems. In Section 4, the novel deterministic model with nonlinear classifier is introduced for both binary and multiclass classification. Section 5 considers the robust extension together with the construction of the uncertainty sets. In Section 6, the computational results are shown. Finally, Section 7 concludes the paper and discusses future works.

2. Literature review

The nonlinear SVM approach presented in Boser et al. (1992) has been explored in several works, leading to alternative formulations. In Mangasarian (1998); Lee et al. (2000) a kernel-induced decision boundary is derived by considering quadratic and piecewise-linear objective function, resulting in a convex model. In Schölkopf et al. (2000) the formulation of ν -Support Vector Classification (ν -SVC) is proposed for both linear and nonlinear classifiers. This algorithm differs from the classical SVM paradigm of Vapnik (1995) since it involves a new parameter ν in the objective function, controlling the number of support vectors. In Jayadeva et al. (2007) the *Twin Support Vector Machine* (TWSVM) is designed. Contrary to standard SVM, TWSVM determines a pair of nonparallel hyperplanes by solving two small-sized SVM-type problems. TWSVM is combined in Peng (2011) with a flexible parametric margin model (Hao (2010)), deriving the *Twin Parametric Margin Support Vector Machine* (TPMSVM). Recently, in Blanco et al. (2020) the classical ℓ_2 -norm problem has been extended to the general case of ℓ_p -norm with $p > 1$, resulting in Second-Order Cone Programming (SOCP, Maggioni et al. (2009)) formulations. The problem of

feature selection in nonlinear SVM is explored in Jiménez-Cordero et al. (2021). The authors propose a method based on a min-max optimization problem, embedding a trade-off between model complexity and classification accuracy.

In order to prevent low accuracies when training data are plagued by uncertainty, RO techniques are applied in the SVM context. In Bhattacharyya (2004) hyperellipsoids around data points are considered, and the robust model results in a SOCP problem. A tractable robust counterpart of the classical SM-SVM approach is derived in Bertsimas et al. (2019). The authors robustify the model by considering additive and bounded-by-norm perturbations in the training data. In El Ghaoui et al. (2003) the binary classification problem under feature uncertainty is formulated with uncertainty sets in the form of hyperrectangles and hyperellipsoids around input data. The same choices of uncertainty sets is made in Faccini et al. (2022), where the RO extension of the linear SVM variant presented in Liu & Potra (2009) is proposed. The reader is referred to Wang & Pardalos (2014) for a survey on linear SVM model under uncertainty.

As far as it concerns RO techniques applied to nonlinear SVM, various approaches exist in the literature. In Bhadra et al. (2010); Ben-Tal et al. (2012) the kernel matrix is assumed to be affected by uncertainty, due to feature perturbations in the input data. Such matrix is decomposed as a linear combination of positive semidefinite matrices with bounded-by- ℓ_p -norm coefficients. The main limitation of this approach is that the functional form of the matrices in the combination is typically unknown. Thus, it is not obvious how to characterize the elements in the uncertainty set, unless by using a sampling procedure. In Bi & Zhang (2005); Trafalis & Gilbert (2006) training data points are subject to uncertain but bounded-by- ℓ_p -norm perturbations. Robustified models are derived for both linear and nonlinear classifiers. In the latter case, only the Gaussian kernel is explored. A related work on bounded-by-norm uncertainty sets is Xu et al. (2009), where a link between regularization and robustness is provided. In Trafalis & Alwazzi (2010) the stability of SVM models with bounded perturbations is investigated by using discriminant functions. Polyhedral uncertainty sets are considered in Fan et al. (2014); Ju & Tian (2012); Fung et al. (2002), based on the nonlinear classifier proposed in Mangasarian (1998).

RO techniques are also applied to variants of the classical SVM model. In Peng & Xu (2013) a robust TWSVM classifier is proposed, by including uncertainty in the variance matrices of the two classes. In Qi et al. (2013) the robust extension of TWSVM is derived. For the nonlinear case, only Gaussian kernel and ellipsoidal uncertainty sets are considered, resulting in SOCP formulation. In De Leone et al. (2023) the robust and multiclass extension of the TPMSVM is provided. A complete survey on recent developments on TWSVM models can be found in Tanveer et al. (2022).

When information on the probability distribution of the training data are available, RO is combined with *Chance-Constrained Programming* (CCP) and *Distributionally Robust Optimization* (DRO) (Ketkov (2024); Jiang & Peng (2024)). The *Minimax Probability Machine* (MPM) is the first robust approach in the SVM context that minimizes the worst-case probability of misclassification (Lanckriet et al. (2002)). In Maldonado et al. (2020) the MPMs are extended and applied to the robust profit-driven churn prediction. Within the MPM framework, the use of Cobb-Douglas function for maximizing the expected class accuracies under a worst-case distribution setting is proposed in Maldonado et al. (2022). The problem of robust feature selection with CCP is explored in López et al. (2018) by using difference of convex functions. Within the multi-

class context, in López et al. (2017) a robust formulation for multiclass classification via TWSVM is proposed. As far as it concerns DRO methods applied to SVM, we mention the recent work of Faccini et al. (2022) where a moment-based distributionally robust extension of the Liu & Potra (2009) formulation is designed. Finally, a combination of CCP and DRO techniques applied to linear SVMs with uncertain data is explored in Wang et al. (2018b); Khanjani-Shiraz et al. (2023).

All the approaches discussed so far are listed in Table 1. For a comprehensive review of RO techniques applied to SVM models the reader is referred to Singla et al. (2020).

The contribution of this paper differs from the literature described above in several aspects. First of all, we present a novel optimization model with nonlinear classifiers, extending the approach of Liu & Potra (2009), both in the case of binary and multiclass classification. Secondly, we consider general bounded-by- ℓ_p -norm uncertainty sets around training observations. This increases the flexibility of the model, adapting the formulation to more complex perturbations in input data. In addition, it results in a generalization of the robust approach of Faccini et al. (2022) where only box and ellipsoidal uncertainty sets have been considered. Thirdly, we derive closed-form expressions of the bounds in the feature space for some of typically used kernel functions in ML literature. Finally, we deduce the robust counterpart of the deterministic formulations, protecting the models against data uncertainty.

		Vapnik & Chervonnensis (1974)	Boer et al. (1992)	Vapnik (1995)	Mangasarian (1998)	Lee et al. (2000)	Schölkopf et al. (2000)	Fung et al. (2002)	Lanckriet et al. (2002)	El Ghoui et al. (2003)	Bhattacharyya (2004)	Bi & Zhang (2005)	Trafalis & Gilbert (2006)	Jayadeva et al. (2007)	Lin & Potra (2009)	Xu et al. (2009)	Bhadra et al. (2010)	Trafalis & Alvaraz (2010)	Peng (2011)	Ben-Tal et al. (2012)	Ju & Tian (2012)	Peng & Xu (2013)	Qi et al. (2013)	Fan et al. (2014)	López et al. (2017)	López et al. (2018)	Wang et al. (2018b)	Berisimas et al. (2019)	Blanco et al. (2020)	Maldonado et al. (2020)	Jiménez-Cordero et al. (2021)	Faccini et al. (2022)	Maldonado et al. (2022)	De Lener et al. (2023)	Khanjani-Shiraz et al. (2023)		
SVM	Linear classifier	✓	✓	✓	✓	✓	✓	✓	✓	✓	✓	✓	✓	✓	✓	✓	✓	✓	✓	✓	✓	✓	✓	✓	✓	✓	✓	✓	✓	✓	✓	✓	✓	✓	✓	✓	
	Nonlinear classifier		✓	✓	✓	✓	✓	✓	✓	✓	✓	✓	✓	✓	✓	✓	✓	✓	✓	✓	✓	✓	✓	✓	✓	✓	✓	✓	✓	✓	✓	✓	✓	✓	✓	✓	
Type of	Box RO						✓																														
	Ellipsoidal RO							✓	✓	✓													✓														
Robust	Polyhedral RO						✓														✓																
	Bounded-by-norm RO											✓	✓																								
Methodology	Matrix RO																✓	✓				✓															
	Chance-Constrained							✓									✓								✓	✓	✓							✓	✓		✓
	Distributionally RO						✓																														

Table 1: A selected SVM literature review. In the first row of the table the methodological contributions are listed in chronological order. Second and third rows specify the type of SVM classifier (linear or nonlinear). Finally, the RO methodologies employed in the articles are explored in rows four to ten.

3. Background and notation

In this section, we report the notation (Section 3.1) and briefly recall the methods that are relevant for our proposal (Section 3.2).

3.1. Notation

In the following, the set of nonnegative real numbers will be denoted by \mathbb{R}^+ , whereas if zero is excluded we write \mathbb{R}_0^+ . Hereinafter, all vectors will be column vectors, unless transposition by the superscript “ \top ”. If a is a vector in \mathbb{R}^n , then its i -th component will be denoted by a_i . The scalar product in a inner product space \mathcal{H} will be denoted by $\langle \cdot, \cdot \rangle$. If $\mathcal{H} = \mathbb{R}^n$ and $a, b \in \mathbb{R}^n$, the dot product will be indifferently denoted as $a^\top b$ or $\langle a, b \rangle$. For $p \in [1, \infty]$, $\|a\|_p$ is the ℓ_p -norm of a . Finally, if $c \in \mathbb{R}$, the indicator function $\mathbb{1}(c)$ has value 1 if c is positive and 0 otherwise. By convention, we assume that $\frac{1}{\infty} := 0$ and $\|a\|_\infty^\infty := \|a\|_\infty$.

3.2. A selected review of SVM models

Let $\{(x^{(i)}, y^{(i)})\}_{i=1}^m$ be the set of training data points, where $x^{(i)} \in \mathbb{R}^n$ is the vector of features, and $y^{(i)} \in \{-1, +1\}$ is the label representing the class to which the i -th data point belongs. In particular, we denote by \mathcal{A} and \mathcal{B} the *positive* (label “+1”) and *negative* (label “-1”) classes, respectively.

The *Soft Margin*-SVM approach (SM-SVM, Cortes & Vapnik (1995)) finds the best separating hyperplane $H := (w, \gamma)$ defined by the equation $w^\top x = \gamma$, where $w \in \mathbb{R}^n$ and $\gamma \in \mathbb{R}$, as solution of the following ℓ_q -model, $q \in [1, \infty]$:

$$\begin{aligned} \min_{w, \gamma, \xi} \quad & \|w\|_q^q + \nu \sum_{i=1}^m \xi_i \\ \text{s.t.} \quad & y^{(i)}(w^\top x^{(i)} - \gamma) \geq 1 - \xi_i \quad i = 1, \dots, m \\ & \xi_i \geq 0 \quad i = 1, \dots, m. \end{aligned} \tag{1}$$

The vector $\xi \in \mathbb{R}^m$ is the soft margin error vector and $\nu \geq 0$ is a regularization parameter. Data point $x^{(i)}$ is correctly classified by the separating hyperplane H if $0 \leq \xi_i \leq 1$, otherwise is misclassified.

Whenever a new observation $x \in \mathbb{R}^n$ occurs, it is classified as *positive* or *negative* depending on the decision function $\mathbb{1}(w^\top x - \gamma)$.

Instead of a single hyperplane, in Liu & Potra (2009) a pair of parallel hyperplanes $H_{\mathcal{A}}$ and $H_{\mathcal{B}}$ is constructed, satisfying the following properties:

- (P1) all points of class \mathcal{A} lie on one halfspace of $H_{\mathcal{A}}$;
- (P2) all points of class \mathcal{B} lie on the opposite halfspace of $H_{\mathcal{B}}$;
- (P3) the intersection of the convex hulls of \mathcal{A} and \mathcal{B} is contained in the region between $H_{\mathcal{A}}$ and $H_{\mathcal{B}}$.

The starting point of the formulation consists in solving the SM-SVM model (1) with $q = 1$, determining an initial separating hyperplane $H_0 := (w, \gamma)$ and the soft margin vector ξ . Then, H_0 is shifted in order to identify $H_{\mathcal{A}} := (w, \gamma - 1 + \omega_{\mathcal{A}})$ and $H_{\mathcal{B}} := (w, \gamma + 1 - \omega_{\mathcal{B}})$, where:

$$\omega_{\mathcal{A}} := \max_{i: x^{(i)} \in \mathcal{A}} \{\xi_i\}, \quad \omega_{\mathcal{B}} := \max_{i: x^{(i)} \in \mathcal{B}} \{\xi_i\}. \tag{2}$$

The choice of $\omega_{\mathcal{A}}$ and $\omega_{\mathcal{B}}$ according to condition (2) guarantees that $H_{\mathcal{A}}$ and $H_{\mathcal{B}}$ satisfy properties (P1)-(P3).

Finally, the optimal separating hyperplane $H := (w, b)$ is such that is parallel to $H_{\mathcal{A}}$ and $H_{\mathcal{B}}$, lies in their strip, and the number of misclassified points is minimized. These conditions are satisfied finding the optimal parameter b as solution of the following problem:

$$\begin{aligned} \min_b \quad & \sum_{i: x^{(i)} \in \mathcal{A}} \mathbb{1}(w^\top x^{(i)} - b) + \sum_{i: x^{(i)} \in \mathcal{B}} \mathbb{1}(b - w^\top x^{(i)}) \\ \text{s.t.} \quad & \gamma + 1 - \omega_{\mathcal{B}} \leq b \leq \gamma - 1 + \omega_{\mathcal{A}}. \end{aligned} \tag{3}$$

From a computational perspective, model (3) is solved through a linear search procedure. Specifically, the interval $[\gamma + 1 - \omega_{\mathcal{B}}, \gamma - 1 + \omega_{\mathcal{A}}]$ is divided into N_{\max} sub-intervals of equal length

and the problem is solved on each of them. The optimal solution b is the one providing the overall minimum value of the objective function.

Similarly to SM-SVM, a new data point $x \in \mathbb{R}^n$ is classified in class \mathcal{A} or \mathcal{B} depending on the decision rule $\mathbb{1}(w^\top x - b)$.

Whenever training observations are not linearly separable, the so-called *kernel trick* can be applied (Cortes & Vapnik (1995)). The key idea is to introduce a function $\phi(\cdot)$, usually referred to as *feature map*, to translate data from the *input space* \mathbb{R}^n to a higher-dimensional space \mathcal{H} , equipped with the dot product $\langle \cdot, \cdot \rangle$. In \mathcal{H} , the transformed data $\{\phi(x^{(i)})\}_{i=1}^m$ are assumed to be linearly separable. Thus, model (1) can be written in the feature space \mathcal{H} as:

$$\begin{aligned} \min_{\bar{w}, \gamma, \xi} \quad & \|\bar{w}\|_{\mathcal{H}} + \nu \sum_{i=1}^m \xi_i \\ \text{s.t.} \quad & y^{(i)}(\langle \bar{w}, \phi(x^{(i)}) \rangle - \gamma) \geq 1 - \xi_i \quad i = 1, \dots, m \\ & \xi_i \geq 0 \quad i = 1, \dots, m. \end{aligned} \tag{4}$$

Vector $\bar{w} \in \mathcal{H}$ defines the linear classifier in the feature space and the norm $\|\cdot\|_{\mathcal{H}}$ is induced by the inner product $\langle \cdot, \cdot \rangle$.

Unfortunately, the expression of the mapping $\phi(\cdot)$ is usually unknown and, consequently, model (4) cannot be solved in practice. To overcome this limitation, a symmetric and positive semidefinite kernel $k : \mathbb{R}^n \times \mathbb{R}^n \rightarrow \mathbb{R}$ is introduced. Examples of kernel functions typically used in ML literature are reported in Table 2. For a comprehensive overview, the reader is referred to Schölkopf & Smola (2001).

Kernel function	$k(x, x')$	Parameter
Homogeneous polynomial	$k(x, x') = \langle x, x' \rangle^d$	$d \in \mathbb{N}$
Inhomogeneous polynomial	$k(x, x') = (c + \langle x, x' \rangle)^d$	$c \in \mathbb{R}^+, d \in \mathbb{N}$
Gaussian Radial Basis Function (RBF)	$k(x, x') = \exp\left(-\frac{\ x - x'\ _2^2}{2\alpha^2}\right)$	$\alpha \in \mathbb{R}_0^+$

Table 2: Examples of kernel functions. The first column reports the name of the functions. The second column provides their mathematical expressions. Finally, the third column contains the related relevant parameters.

As in Cortes & Vapnik (1995), \bar{w} can be decomposed into a finite linear combination of $\{\phi(x^{(j)})\}_{j=1}^m$, as $\bar{w} = \sum_{j=1}^m y^{(j)} u_j \phi(x^{(j)})$, for some coefficients $u_j \in \mathbb{R}$. Consequently, for all $i = 1, \dots, m$ the dot product $\langle \bar{w}, \phi(x^{(i)}) \rangle$ in the first set of constraints of model (4) can be formulated as $\langle \bar{w}, \phi(x^{(i)}) \rangle = \sum_{j=1}^m K_{ij} y^{(j)} u_j$, where $K_{ij} := k(x^{(i)}, x^{(j)}) = \langle \phi(x^{(i)}), \phi(x^{(j)}) \rangle$. The properties of the kernel function imply that the Gram matrix $K = [K_{ij}]$ is a real, symmetric and positive semidefinite $m \times m$ matrix (Piccialli & Sciandrone (2018)).

As in Mangasarian (1998); Lee et al. (2000), in the objective function of model (4) $\|\bar{w}\|_{\mathcal{H}}$ is replaced by $\|u\|_q^q$, where $u := [u_1, \dots, u_m]^\top$. This choice guarantees the convexity of the optimization

problem. Therefore, model (4) can be rewritten as:

$$\begin{aligned}
\min_{u, \gamma, \xi} \quad & \|u\|_q^q + \nu \sum_{i=1}^m \xi_i \\
\text{s.t.} \quad & y^{(i)} \left(\sum_{j=1}^m K_{ij} y^{(j)} u_j - \gamma \right) \geq 1 - \xi_i \quad i = 1, \dots, m \\
& \xi_i \geq 0 \quad i = 1, \dots, m.
\end{aligned} \tag{5}$$

Within this context, the separating hyperplane in the feature space translates into a nonlinear decision boundary $S := (u, \gamma)$ in the input space, defined by the following equation:

$$\sum_{i=1}^m k(x, x^{(i)}) y^{(i)} u_i = \gamma. \tag{6}$$

Finally, each new observation $x \in \mathbb{R}^n$ is classified either in class \mathcal{A} or \mathcal{B} according to the decision function $\mathbb{1}(\sum_{i=1}^m k(x, x^{(i)}) y^{(i)} u_i - \gamma)$.

4. A novel approach for deterministic nonlinear SVM

In this section, we propose an extension of the SVM approach presented in Liu & Potra (2009) to the nonlinear case. Specifically, we classify input observations by means of kernel-induced decision boundaries, such that the corresponding hyperplanes in the feature space satisfy properties **(P1)**-**(P3)**.

In Section 4.1 we tackle a binary classification task, whereas in Section 4.2 we extend the approach to the case of multiclass classification.

4.1. Binary classification

First of all, we start solving model (5) and finding an initial decision boundary $S_0 := (u, \gamma)$. In the input space, hypersurface S_0 induces an initial nonlinear separation of training data points. Accordingly, in the feature space the corresponding hyperplane H_0 performs a linear classification of transformed observations.

Then, for each of the two classes, we compute the greatest misclassification error through the extended version of formulas (2):

$$\omega_{\mathcal{A}} := \max_{i=1, \dots, m} (D\xi)_i \quad \omega_{\mathcal{B}} := \max_{i=1, \dots, m} (-D\xi)_i, \tag{7}$$

where D is a diagonal matrix with entries $D_{ii} := y^{(i)}$, for all $i = 1, \dots, m$.

Due to the structure of problem (5), the modulus of $-1 + \omega_{\mathcal{A}}$ represents the deviation of the farthest misclassified point of class \mathcal{A} from H_0 and similarly for $1 - \omega_{\mathcal{B}}$. Nevertheless, it may happen that H_0 already correctly classifies all the data points of one or both classes. In that case, the moduli are just the deviations of the closest data points from hyperplane H_0 . According to the classic literature of SVM (see Cortes & Vapnik (1995)), we call *support vectors* of class \mathcal{A} and \mathcal{B} the transformed points that deviate $|-1 + \omega_{\mathcal{A}}|$ and $|1 - \omega_{\mathcal{B}}|$ from H_0 , respectively.

At this stage, similarly to Liu & Potra (2009), we shift hyperplane H_0 by $-1 + \omega_{\mathcal{A}}$ and $1 - \omega_{\mathcal{B}}$, obtaining $H_{\mathcal{A}}$ and $H_{\mathcal{B}}$, respectively. Such a pair of parallel hyperplanes passes through the support vectors of the corresponding class and satisfies properties **(P1)**-**(P3)** in the feature space. According to equation (6), the corresponding hypersurfaces $S_{\mathcal{A}} := (u, \gamma - 1 + \omega_{\mathcal{A}})$ and $S_{\mathcal{B}} := (u, \gamma + 1 - \omega_{\mathcal{B}})$ are then derived in the input space.

Finally, the optimal kernel-induced decision boundary $S := (u, b)$ is deduced, where b is the solution of the nonlinear version of model (3):

$$\begin{aligned} \min_b \quad & \sum_{i=1}^m \mathbb{1} \left(y^{(i)} b - y^{(i)} \sum_{j=1}^m K_{ij} y^{(j)} u_j \right) \\ \text{s.t.} \quad & \gamma + 1 - \omega_{\mathcal{B}} \leq b \leq \gamma - 1 + \omega_{\mathcal{A}}. \end{aligned} \tag{8}$$

We observe that hypersurface S in the input space is induced by hyperplane H in the feature space, which is parallel to $H_{\mathcal{A}}$ and $H_{\mathcal{B}}$ and lies in the region between them. Therefore, a new observation $x \in \mathbb{R}^n$ is classified according to the decision function $\mathbb{1}(\sum_{i=1}^m k(x, x^{(i)}) y^{(i)} u_i - b)$.

For the sake of clarity, all the steps of the approach discussed so far are schematically reported in Pseudocode 1.

Pseudocode 1 A novel approach for nonlinear SVM.

Input: $\{(x^{(i)}, y^{(i)})\}_{i=1}^m$, $q \in [1, \infty]$, $\nu \geq 0$, $k(\cdot, \cdot) : \mathbb{R}^n \times \mathbb{R}^n \rightarrow \mathbb{R}$.

- 1: Calculate matrix K as $K_{ij} = k(x^{(i)}, x^{(j)})$, $i, j = 1, \dots, m$.
- 2: Solve model (5).
- 3: Find the initial separating hypersurface $S_0 = (u, \gamma)$, defined by equation (6).
- 4: Construct diagonal matrix D as $D_{ii} = y^{(i)}$, $i = 1, \dots, m$, and compute $\omega_{\mathcal{A}}$ and $\omega_{\mathcal{B}}$ according to formulas (7).
- 5: Shift S_0 to get the separating hypersurface for each class, $S_{\mathcal{A}} = (u, \gamma - 1 + \omega_{\mathcal{A}})$ and $S_{\mathcal{B}} = (u, \gamma + 1 - \omega_{\mathcal{B}})$, defined by (6).
- 6: Solve model (8), obtaining parameter b .

Output: The optimal decision boundary $S = (u, b)$, defined by (6).

The computational complexity of nonlinear SVM models is between $O(m^2)$ and $O(m^3)$ (Peng (2011)). Since model (8) requires at most N_{\max} iterations to be solved through a linear search procedure, the computational complexity of our approach is between $O(\max\{m^2, N_{\max}\})$ and $O(\max\{m^3, N_{\max}\})$.

By way of illustration, in Figure 1 we depict the separating surfaces obtained by applying the proposed SVM methodology to a bidimensional toy example. In model (5) we set $q = 1$, $\nu = 1$ and consider linear and Gaussian RBF kernels. The graphical interpretation of the novel approach is illustrated in Figure 2.

4.2. Multiclass classification

In this section, we derive the multiclass extension of the approach presented so far. We focus our attention on one of the most commonly used multiclass SVM framework, the *one-versus-all* (Vapnik (1995)). According to this methodology, L binary classifiers are constructed, where L

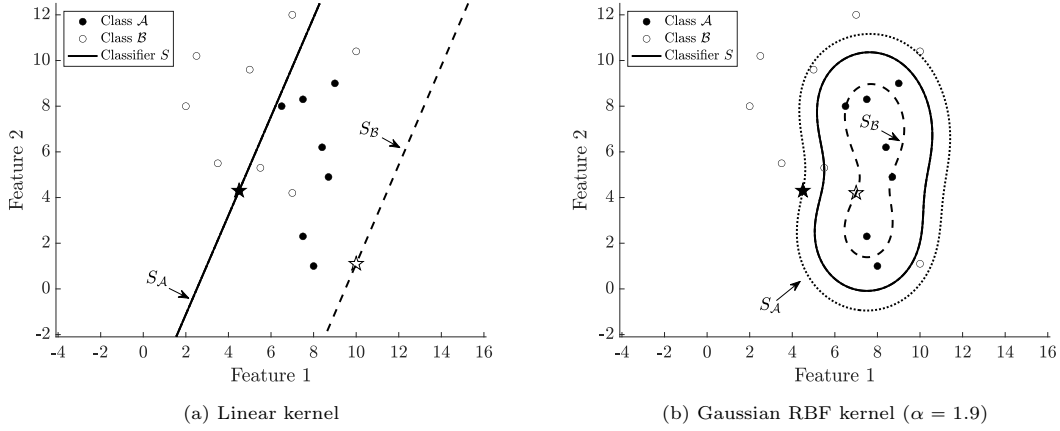


Figure 1: Separating surfaces obtained with linear and Gaussian RBF kernel functions. Support vectors are depicted as stars.

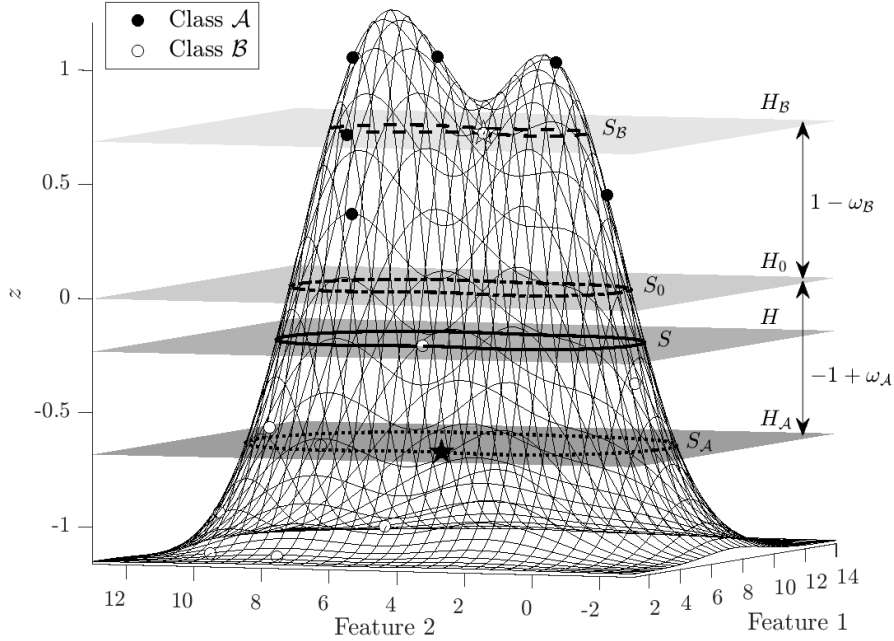


Figure 2: Graphical representation of the implicit function (6), in the case of Gaussian RBF kernel ($\alpha = 1.9$), along with the separating hyperplanes and decision boundaries. Support vectors are drawn as stars.

is the number of classifying categories, such that each class is independently separated by all the others grouped together. Formally, let $\{(x^{(i)}, y^{(i)})\}_{i=1}^m$ be the set of training observations, with $x^{(i)} \in \mathbb{R}^n$ and $y^{(i)} \in \{1, \dots, L\}$. For each class $l = 1, \dots, L$, we find an initial separating hypersurface $S_{l,0} := (u_l, \gamma_l)$, where $u_l \in \mathbb{R}^n$ and $\gamma_l \in \mathbb{R}$ are the solutions of the following multiclass

version of model (5):

$$\begin{aligned}
\min_{u_l, \gamma_l, \xi_l} \quad & \|u_l\|_q^q + \nu \sum_{i=1}^m \xi_{l,i} \\
\text{s.t.} \quad & \hat{y}_l^{(i)} \left(\sum_{j=1}^m K_{ij} \hat{y}_l^{(j)} u_{l,j} - \gamma_l \right) \geq 1 - \xi_{l,i} \quad i = 1, \dots, m \\
& \xi_{l,i} \geq 0 \quad i = 1, \dots, m,
\end{aligned} \tag{9}$$

with $\hat{y}_l^{(i)} = 1$ if $y^{(i)} = l$, and $\hat{y}_l^{(i)} = -1$ otherwise. Then, we construct the diagonal matrix \hat{D}_l , with $\hat{D}_{l,ii} := \hat{y}_l^{(i)}$, $i = 1, \dots, m$, and compute:

$$\omega_l := \max_{i=1, \dots, m} (\hat{D}_l \xi_l)_i \quad \omega_{-l} := \max_{i=1, \dots, m} (-\hat{D}_l \xi_l)_i.$$

Hypersurface $S_{l,0}$ is then shifted to get $S_l := (u_l, \gamma_l - 1 + \omega_l)$ and $S_{-l} := (u_l, \gamma_l + 1 - \omega_{-l})$ in the input space. The corresponding hyperplanes in the feature space satisfy properties **(P1)**-**(P3)**. Finally, the optimal decision boundary for class l versus all the others is $S_{l,-l} := (u_l, b_l)$, with b_l solution of the following model:

$$\begin{aligned}
\min_{b_l} \quad & \sum_{i=1}^m \mathbb{1} \left(\hat{y}_l^{(i)} b_l - \hat{y}_l^{(i)} \sum_{j=1}^m K_{ij} \hat{y}_l^{(j)} u_{l,j} \right) \\
\text{s.t.} \quad & \gamma_l + 1 - \omega_{-l} \leq b_l \leq \gamma_l - 1 + \omega_l.
\end{aligned} \tag{10}$$

The decision function of the l -th class is given by $f_l(x) := \sum_{i=1}^m k(x, x^{(i)}) \hat{y}_l^{(i)} u_{l,i} - b_l$, and each new observation $x \in \mathbb{R}^n$ is assigned to the class $l^* := \arg \max_{l=1, \dots, L} f_l(x)$ (López et al. (2017)).

Since the *one-versus-all* strategy generates L binary classifiers, one for each class, the computational complexity of our multiclass approach is between $O(L \cdot \max\{m^2, N_{\max}\})$ and $O(L \cdot \max\{m^3, N_{\max}\})$.

We represent in Figure 3 the results of the proposed methodology in the case of a multiclass classification task. The parameters q and ν are the same as in Figure 1. Similarly to the binary case (see Figure 1a), it may happen that either S_l or S_{-l} coincides with $S_{l,-l}$. This is due to the fact that in model (10) the optimal parameter b_l may be equal to $\gamma_l - 1 + \omega_l$ or $\gamma_l + 1 - \omega_{-l}$, respectively.

5. A robust model for nonlinear SVM

In this section, we derive the robust counterpart of the deterministic approach discussed so far, when input data are plagued by uncertainties. According to the RO framework, we construct an uncertainty set around each observation and optimize against the worst-case realization across the entire uncertainty set (Bertsimas et al. (2019)).

Contrariwise to RO models dealing with linear classification (see, for instance, Faccini et al. (2022)), in the nonlinear context data points $x^{(i)}$ are mapped into the feature space \mathcal{H} via $\phi(\cdot)$ and uncertainty sets $\mathcal{U}_{\mathcal{H}}(\phi(x^{(i)}))$ have to be constructed. Unfortunately, a closed-form expression

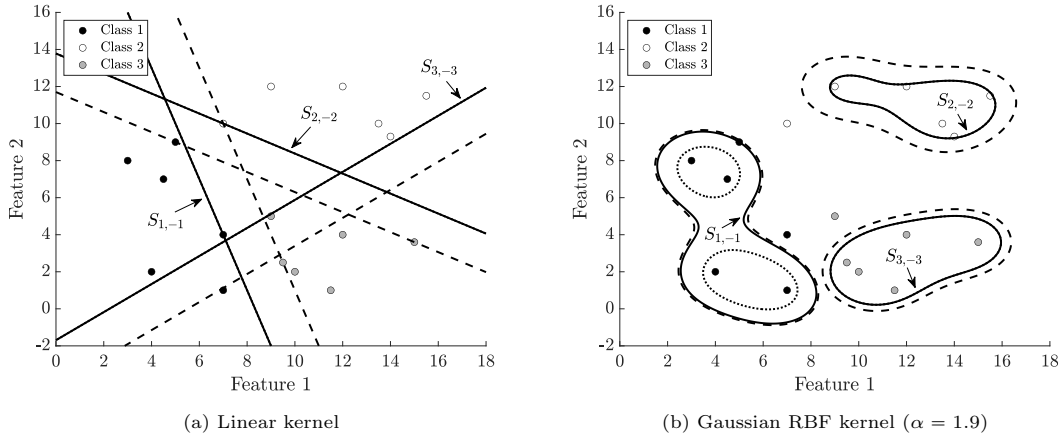


Figure 3: Separating surfaces obtained with linear and Gaussian RBF kernel functions in the case of a three-classes classification task. For each class $l = 1, 2, 3$, the dotted line and the dashed line represent respectively S_l and S_{-l} .

of $\phi(\cdot)$ is rarely available and an *a priori* control about $\mathcal{U}_{\mathcal{H}}(\phi(x^{(i)}))$ is not possible. Therefore, further assumptions on the uncertainty set $\mathcal{U}_{\mathcal{H}}(\phi(x^{(i)}))$ in the feature space are necessary.

The remainder of the section is organized as follows. In Section 5.1 bounded-by- ℓ_p -norm uncertainty sets $\mathcal{U}_p(x^{(i)})$ are constructed, together with the corresponding ones $\mathcal{U}_{\mathcal{H}}(\phi(x^{(i)}))$ in the feature space. Bounds on the radii of $\mathcal{U}_{\mathcal{H}}(\phi(x^{(i)}))$ are derived in Section 5.2. Finally, in Section 5.3 the robust counterpart of models (5) and (9) is formulated.

5.1. The construction of the uncertainty sets

We assume that each observation $x^{(i)}$ in the input space is subject to an additive and unknown perturbation vector $\sigma^{(i)}$, whose ℓ_p -norm, with $p \in [1, \infty]$, is bounded by a nonnegative constant $\eta^{(i)}$. Consequently, the uncertainty set around $x^{(i)}$ has the following expression:

$$\mathcal{U}_p(x^{(i)}) := \left\{ x \in \mathbb{R}^n : x = x^{(i)} + \sigma^{(i)}, \|\sigma^{(i)}\|_p \leq \eta^{(i)} \right\}. \quad (11)$$

Parameter $\eta^{(i)}$ calibrates the degree of conservatism: if $\eta^{(i)} = 0$, then $\sigma^{(i)}$ is the zero vector of \mathbb{R}^n and $\mathcal{U}_p(x^{(i)})$ coincides with $x^{(i)}$. Popular choices for the ℓ_p -norm in the RO literature are $p = 1, 2, \infty$, leading to polyhedral, spherical and box uncertainty sets, respectively.

In order to consider the extension towards the feature space, we now assume that, if x belongs to $\mathcal{U}_p(x^{(i)})$, then:

$$\phi(x) = \phi(x^{(i)} + \sigma^{(i)}) = \phi(x^{(i)}) + \zeta^{(i)},$$

where the perturbation $\zeta^{(i)}$ belongs to the feature space \mathcal{H} and its \mathcal{H} -norm is bounded a nonnegative constant $\delta^{(i)}$. The latter may be unknown but it depends on the known bound $\eta^{(i)}$ in the input space, i.e. $\delta^{(i)} = \delta^{(i)}(\eta^{(i)})$. If no uncertainty occurs in the input space, no uncertainty will occur in the feature space too: $\eta^{(i)} = 0$ implies $\delta^{(i)} = 0$. Hence, the uncertainty set around $\phi(x^{(i)})$ in the feature space is modelled as:

$$\mathcal{U}_{\mathcal{H}}(\phi(x^{(i)})) := \left\{ z \in \mathcal{H} : z = \phi(x^{(i)}) + \zeta^{(i)}, \|\zeta^{(i)}\|_{\mathcal{H}} \leq \delta^{(i)} \right\}. \quad (12)$$

5.2. Bounds on the uncertainty sets in the feature space

Let $k(\cdot, \cdot)$ be a symmetric and positive semidefinite kernel, with corresponding feature map $\phi(\cdot)$. In the following, we derive closed-form expressions for the radius $\delta^{(i)}$ in the feature space given the bound $\eta^{(i)}$ in the input space, when $k(\cdot, \cdot)$ is the polynomial kernel or the Gaussian RBF kernel. Below, we provide the results and relegate the proofs to Appendix A.

Proposition 1 (Polynomial kernel). Let $\mathcal{U}_p(x^{(i)})$ and $\mathcal{U}_{\mathcal{H}}(\phi(x^{(i)}))$ be the uncertainty sets in the input and in the feature space as in (11) and (12), respectively, with $p \in [1, \infty]$. Consider the inhomogeneous polynomial kernel of degree $d \in \mathbb{N}$ and additive constant $c \geq 0$, with radius $\delta^{(i)} \equiv \delta_{d,c}^{(i)}$ and:

$$C = C(n, p) = \begin{cases} 1, & 1 \leq p \leq 2 \\ n^{\frac{p-2}{2p}}, & p > 2. \end{cases}$$

(i) If $d = 1$, then the radius of $\mathcal{U}_{\mathcal{H}}(\phi(x^{(i)}))$ is:

$$\delta_{1,c}^{(i)} = C\eta^{(i)}. \quad (13)$$

(ii) If $d > 1$, then:

$$\delta_{d,c}^{(i)} = \sqrt{(\delta_{d,0}^{(i)})^2 + \sum_{k=1}^{d-1} \binom{d}{k} c^k \left[\sum_{j=1}^{d-k} \binom{d-k}{j} \|x^{(i)}\|_2^{d-k-j} (C\eta^{(i)})^j \right]^2}, \quad (14)$$

where $\delta_{d,0}^{(i)}$ is the bound for the corresponding homogeneous polynomial kernel:

$$\delta_{d,0}^{(i)} = \sum_{k=1}^d \binom{d}{k} \|x^{(i)}\|_2^{d-k} (C\eta^{(i)})^k. \quad (15)$$

Notice that when $c = 0$, equation (14) reduces to (15).

Proposition 2 (Gaussian RBF kernel). Let $\mathcal{U}_p(x^{(i)})$ and $\mathcal{U}_{\mathcal{H}}(\phi(x^{(i)}))$ be the uncertainty sets in the input and in the feature space as in (11) and (12), respectively, with $p \in [1, \infty]$. Consider the Gaussian RBF kernel with parameter $\alpha > 0$ and radius $\delta^{(i)} \equiv \delta_{\alpha}^{(i)}$. If:

$$C = C(n, p) = \begin{cases} 1, & 1 \leq p \leq 2 \\ n^{\frac{p-2}{2p}}, & p > 2, \end{cases}$$

then:

$$\delta_{\alpha}^{(i)} = \sqrt{2 - 2 \exp\left(-\frac{(C\eta^{(i)})^2}{2\alpha^2}\right)}. \quad (16)$$

We observe that Propositions 1-2 are consistent with Lemma 7 presented in Xu et al. (2009). However, in this paper we specify the bounds for particular choices of the kernel functions. In addition, we extend the result for a bounded-by- ℓ_p -norm uncertainty set for a generic $p \in [1, \infty]$.

Then, the modulus of the objective function of model (21) can be bounded by $\sum_{j=1}^m |\langle \zeta^{(i)}, \phi(x^{(j)}) \rangle| \cdot |u_j|$. By applying the Cauchy-Schwarz inequality in \mathcal{H} and the boundedness condition on $\|\zeta^{(i)}\|_{\mathcal{H}}$, we get:

$$\left| \langle \zeta^{(i)}, \phi(x^{(j)}) \rangle \right| \leq \|\zeta^{(i)}\|_{\mathcal{H}} \cdot \|\phi(x^{(j)})\|_{\mathcal{H}} \leq \delta^{(i)} \cdot \sqrt{\langle \phi(x^{(j)}), \phi(x^{(j)}) \rangle} = \delta^{(i)} \cdot \sqrt{K_{jj}}.$$

The value K_{jj} is nonnegative, due to the positive semidefiniteness of the Gram matrix K . Therefore, we obtain:

$$\left| y^{(i)} \sum_{j=1}^m \langle \zeta^{(i)}, \phi(x^{(j)}) \rangle y^{(j)} u_j \right| \leq \delta^{(i)} \sum_{j=1}^m \sqrt{K_{jj}} |u_j|. \quad (22)$$

Thus, the optimal value of model (21) is $-\delta^{(i)} \sum_{j=1}^m \sqrt{K_{jj}} |u_j|$. By replacing the minimization term with this optimal value in the first set of constraints of (19), the thesis follows. \square

When no uncertainty occurs in the data, $\delta^{(i)} = 0$ for all $i = 1, \dots, m$ and the robust model (18) reduces to the deterministic formulation (5).

Model (18) is a convex nonlinear optimization model due to the presence of the ℓ_q -norm of u . Nevertheless, it can be reformulated as a *Linear Programming* (LP) problem when $q = 1$ or $q = \infty$ and as a SOCP problem when $q = 2$, as stated in the following result. The proof is provided in Appendix A.

Corollary 1. Model (18) can be expressed as a LP problem or as a SOCP problem in the following cases:

a) Case $q = 1$: LP problem

$$\begin{aligned} \min_{u, \gamma, \xi, s} \quad & \sum_{i=1}^m s_i + \nu \sum_{i=1}^m \xi_i \\ \text{s.t.} \quad & y^{(i)} \sum_{j=1}^m K_{ij} y^{(j)} u_j - \delta^{(i)} \sum_{j=1}^m \sqrt{K_{jj}} s_j \geq 1 - \xi_i + y^{(i)} \gamma \quad i = 1, \dots, m \\ & s_i \geq -u_i \quad i = 1, \dots, m \\ & s_i \geq u_i \quad i = 1, \dots, m \\ & s_i, \xi_i \geq 0 \quad i = 1, \dots, m. \end{aligned} \quad (23)$$

b) Case $q = 2$: SOCP problem

$$\begin{aligned}
\min_{u, \gamma, \xi, s, r, t, v} \quad & r - v + \nu \sum_{i=1}^m \xi_i \\
\text{s.t.} \quad & y^{(i)} \sum_{j=1}^m K_{ij} y^{(j)} u_j - \delta^{(i)} \sum_{j=1}^m \sqrt{K_{jj}} s_j \geq 1 - \xi_i + y^{(i)} \gamma \quad i = 1, \dots, m \\
& t \geq \|u\|_2 \\
& r + v = 1 \\
& r \geq \sqrt{t^2 + v^2} \\
& s_i \geq -u_i \quad i = 1, \dots, m \\
& s_i \geq u_i \quad i = 1, \dots, m \\
& s_i, \xi_i \geq 0 \quad i = 1, \dots, m.
\end{aligned} \tag{24}$$

c) Case $q = \infty$: LP problem

$$\begin{aligned}
\min_{u, \gamma, \xi, s, s_\infty} \quad & s_\infty + \nu \sum_{i=1}^m \xi_i \\
\text{s.t.} \quad & y^{(i)} \sum_{j=1}^m K_{ij} y^{(j)} u_j - \delta^{(i)} \sum_{j=1}^m \sqrt{K_{jj}} s_j \geq 1 - \xi_i + y^{(i)} \gamma \quad i = 1, \dots, m \\
& s_\infty \geq -u_i \quad i = 1, \dots, m \\
& s_\infty \geq u_i \quad i = 1, \dots, m \\
& s_i \geq -u_i \quad i = 1, \dots, m \\
& s_i \geq u_i \quad i = 1, \dots, m \\
& s_\infty \geq 0 \\
& s_i, \xi_i \geq 0 \quad i = 1, \dots, m.
\end{aligned} \tag{25}$$

As in the deterministic setting, once u , γ and ξ are obtained as solutions of model (18), then $\omega_{\mathcal{A}}$ and $\omega_{\mathcal{B}}$ are computed according to formulas (7). Finally, the optimal separating hypersurface $S = (u, b)$ is derived, where b is the optimal solution of the following robust counterpart of problem (8):

$$\begin{aligned}
\min_b \quad & \sum_{i=1}^m \mathbb{1} \left[\left(y^{(i)} b - y^{(i)} \sum_{j=1}^m K_{ij} y^{(j)} u_j + \delta^{(i)} \sum_{j=1}^m \sqrt{K_{jj}} |u_j| \right)_i \right] \\
\text{s.t.} \quad & \gamma + 1 - \omega_{\mathcal{B}} \leq b \leq \gamma - 1 + \omega_{\mathcal{A}}.
\end{aligned} \tag{26}$$

When dealing with a multiclass classification task, the robust extension of model (9) for the

l -th class is given by:

$$\begin{aligned}
\min_{u_l, \gamma_l, \xi_l} \quad & \|u_l\|_q^q + \nu \sum_{i=1}^m \xi_{l,i} \\
\text{s.t.} \quad & \hat{y}_l^{(i)} \sum_{j=1}^m K_{ij} \hat{y}_l^{(j)} u_{l,j} - \delta^{(i)} \sum_{j=1}^m \sqrt{K_{jj}} |u_{l,j}| \geq 1 - \xi_{l,i} + \hat{y}_l^{(i)} \gamma_l \quad i = 1, \dots, m \\
& \xi_{l,i} \geq 0 \quad i = 1, \dots, m.
\end{aligned} \tag{27}$$

The optimal parameter b_l is the solution of:

$$\begin{aligned}
\min_{b_l} \quad & \sum_{i=1}^m \mathbb{1} \left[\left(\hat{y}_l^{(i)} b_l - \hat{y}_l^{(i)} \sum_{j=1}^m K_{ij} \hat{y}_l^{(j)} u_{l,j} + \delta^{(i)} \sum_{j=1}^m \sqrt{K_{jj}} |u_{l,j}| \right)_i \right] \\
\text{s.t.} \quad & \gamma_l + 1 - \omega_{-l} \leq b_l \leq \gamma_l - 1 + \omega_l.
\end{aligned} \tag{28}$$

Since the structural form of the robust models (18) and (27) is the same as their deterministic equivalent, the time complexity analysis provides analogous results.

For the sake of illustration, we depict in Figure 4 the kernel-induced decision boundaries of the robust model (23), considering the same dataset of Figure 1. The model is trained for both spherical (see Figure 4a) and box (see Figure 4b) uncertainty sets.

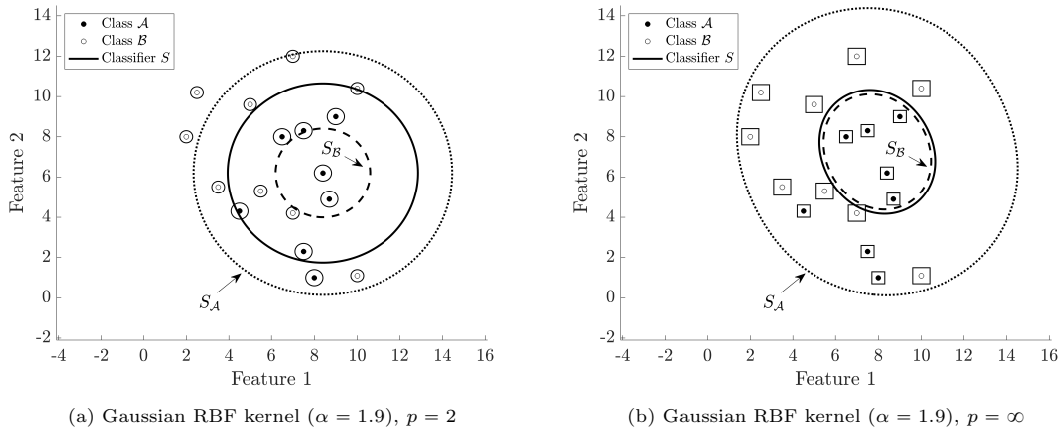


Figure 4: Separating surfaces obtained with Gaussian RBF kernel function from the robust model (23). The ℓ_p -norms defining the uncertainty sets are $p = 2$ (on the left) and $p = \infty$ (on the right).

6. Computational results

In this section, we evaluate the performance of the deterministic models presented in Section 4 and their robust counterparts of Section 5 on a selection of 12 benchmark datasets taken from the UCI Machine Learning Repository (Kelly et al. (2023)). The models were implemented in MATLAB (v. 2021b) and solved using CVX (v. 2.2, see Grant & Boyd (2008, 2014)) and MOSEK solver (v. 9.1.9, see MOSEK ApS (2019)). All computational experiments were run on a MacBookPro17.1 with a chip Apple M1 of 8 cores and 16 GB of RAM memory.

The benchmark datasets are listed in the first column of Table 3, along with the corresponding number of observations m and of features n . In this study we examine 10 binary classification problems and 2 multiclass classification problems.

The experimental setting is as follows. Each dataset was split into *training set*, composed by the $\beta\%$ of the observations, and *testing set*, composed by the remaining $(100 - \beta)\%$. We accounted for three different values of β , leading to the holdouts 75%-25%, 50%-50%, and 25%-75%. The partition was performed inline with the *proportional random sampling* strategy (Chen et al. (2001)), meaning that the original class balance in the entire dataset was maintained in both training and testing set. Once the partition was complete, a kernel function $k(\cdot, \cdot)$ was chosen and the training set used to train the deterministic classifier for different values of input parameter ν . Specifically, the deterministic formulation was solved on five logarithmically spaced values of ν between 10^{-3} and 10^0 using a grid-search strategy, and with $N_{\max} = 10^4$ (see Faccini et al. (2022)). The optimal classifier was chosen among the five candidates as the one minimizing the misclassification error on the training set. Finally, the out-of-sample error on the testing set was computed, as the ratio between the total number of misclassified points in the testing set and its cardinality. In order to get stable results, the partition in training and testing set was performed 96 times in a *repeated holdout* fashion (Kim (2009)). The choice of this number is motivated by the use of the Parallel Computing Toolbox in MATLAB, since the code was parallelized on the 8 cores of the working machine. The final results were then averaged.

As in the original work of Liu & Potra (2009) and in the robust linear extension presented in Faccini et al. (2022), we considered $q = 1$ in the objective function of the models. This choice provides a good compromise between structural risk minimization, related to the misclassification error, and parsimony since it automatically performs feature selection (Labbé et al. (2019); López et al. (2019)).

As far as it concerns the kernel function $k(\cdot, \cdot)$, we tested seven different alternatives: homogeneous linear ($d = 1, c = 0$), homogeneous quadratic ($d = 2, c = 0$), homogeneous cubic ($d = 3, c = 0$); inhomogeneous linear, inhomogeneous quadratic, inhomogeneous cubic; Gaussian RBF. For simplicity, parameter α in the Gaussian RBF kernel was set as the maximum value of the standard deviation across features for the dataset under consideration. Similarly for parameter c in the inhomogeneous polynomial kernels.

Since models (5), (9) and their robust extensions (18), (27) are distance-based, imbalances in the order of magnitude of the features may result in distorted weights when classifying. For this reason, we considered *min-max normalization* and *standardization* as pre-processing techniques of data transformation (Han et al. (2011)). On one hand, in the min-max normalization each dataset was linearly scaled feature-wise into the n -dimensional hypercube $[0, 1]^n$. On the other hand, in the standardization the values of a specific feature j were normalized based on its mean μ_j and standard deviation std_j .

Among all the optimal deterministic classifiers found for each pair *data transformation-kernel function*, the best configuration was chosen as the one minimizing the overall out-of-sample testing error. Within this choice of *data transformation-kernel function*, the robust model was solved. The

bounds $\eta^{(i)}$ on the perturbation vectors defining the uncertainty sets $\mathcal{U}_p(x^{(i)})$ were adjusted as:

$$\begin{aligned}\eta^{(i)} &= \eta_{\mathcal{A}} := \rho_{\mathcal{A}} \max_{j=1,\dots,n} std_{j,\mathcal{A}} & \forall i : x^{(i)} \in \mathcal{A} \\ \eta^{(i)} &= \eta_{\mathcal{B}} := \rho_{\mathcal{B}} \max_{j=1,\dots,n} std_{j,\mathcal{B}} & \forall i : x^{(i)} \in \mathcal{B},\end{aligned}$$

where $\rho_{\mathcal{A}}$ is a nonnegative parameter allowing the user to tailor the degree of conservatism and $\max_{j=1,\dots,n} std_{j,\mathcal{A}}$ is the maximum standard deviation feature-wise for training points of class \mathcal{A} . Similarly for $\rho_{\mathcal{B}}$ and $\max_{j=1,\dots,n} std_{j,\mathcal{B}}$. Once $\eta^{(i)}$ had been determined, the computation of the bound $\delta^{(i)}$ in the feature space was performed according to Propositions 1-2. For simplicity, we set $\rho_{\mathcal{A}} = \rho_{\mathcal{B}} = \rho$, and considered 7 logarithmically spaced values for ρ between 10^{-7} and 10^{-1} . When the number of classes is greater than two, an analogous approach was applied class-wise. As in the deterministic setting, we averaged the out-of-sample testing errors for 96 random partitions of the dataset.

For each dataset, we report in Table 3 the best configuration *data transformation-kernel function*, along with the average out-of-sample testing errors and standard deviations for the deterministic and robust models (holdout 75% training set-25% testing set). We considered three types of uncertainty set, defined respectively by ℓ_1 -, ℓ_2 - and ℓ_∞ -norm. Detailed results are reported in Tables B.7-B.21 in Appendix B.

Dataset $m \times n$	Data transformation	Kernel	Deterministic		Robust		Robust improvement ratio
			$p = 1$	$p = 2$	$p = \infty$		
Arrhythmia 68×279	–	Gaussian RBF	20.47% \pm 0.07	19.12% \pm 0.08	19.30% \pm 0.07	19.61% \pm 0.07	6.60%
CPU time (s)			0.289	0.290	0.288	0.295	
Parkinson 195×22	Min-max normalization	Hom. linear	13.19% \pm 0.03	12.98% \pm 0.03	12.37% \pm 0.03	12.61% \pm 0.04	6.22%
CPU time (s)			3.626	3.421	3.454	3.418	
Heart Disease 297×13	Standardization	Inhom. linear	17.48% \pm 0.04	16.84% \pm 0.04	17.53% \pm 0.03	16.36% \pm 0.04	6.41%
CPU time (s)			12.253	11.602	11.477	11.417	
Dermatology 358×34	–	Inhom. quadratic	1.64% \pm 0.02	1.65% \pm 0.01	1.57% \pm 0.01	0.55% \pm 0.01	66.46%
CPU time (s)			20.173	20.055	20.420	20.147	
Climate Model Crashes 540×18	–	Hom. linear	5.01% \pm 0.02	4.47% \pm 0.02	4.50% \pm 0.01	4.34% \pm 0.01	13.37%
CPU time (s)			68.069	66.762	67.169	67.381	
Breast Cancer Diagnostic 569×30	Min-max normalization	Inhom. quadratic	3.02% \pm 0.02	2.63% \pm 0.01	2.65% \pm 0.01	2.39% \pm 0.01	20.86%
CPU time (s)			77.786	77.968	78.267	77.543	
Breast Cancer 683×9	Standardization	Hom. linear	3.17% \pm 0.01	2.97% \pm 0.01	3.07% \pm 0.01	3.06% \pm 0.01	6.31%
CPU time (s)			135.765	135.651	137.039	136.286	
Blood Transfusion 748×4	Standardization	Inhom. cubic	20.72% \pm 0.02	20.60% \pm 0.02	20.55% \pm 0.02	20.64% \pm 0.02	0.82%
CPU time (s)			178.136	178.751	179.682	180.083	
Mammographic Mass 830×5	Standardization	Inhom. quadratic	15.71% \pm 0.02	15.49% \pm 0.02	15.42% \pm 0.02	15.54% \pm 0.02	1.85%
CPU time (s)			241.205	241.810	242.614	241.929	
Qsar Biodegradation 1055×41	Min-max normalization	Gaussian RBF	12.88% \pm 0.02	11.78% \pm 0.01	12.72% \pm 0.02	12.86% \pm 0.02	8.54%
CPU time (s)			484.908	498.235	495.073	491.748	
Iris 150×4 (3 classes)	–	Gaussian RBF	3.10% \pm 0.03	3.07% \pm 0.03	3.21% \pm 0.03	2.87% \pm 0.03	7.42%
CPU time (s)			5.391	5.684	5.627	5.604	
Wine 178×13 (3 classes)	Standardization	Inhom. linear	2.77% \pm 0.02	2.63% \pm 0.02	2.63% \pm 0.02	2.51% \pm 0.02	9.39%
CPU time (s)			7.916	8.361	8.352	8.605	

Table 3: Average out-of-sample testing errors and standard deviations over 96 runs for the deterministic and robust models. Best results are highlighted. The last column displays the robust improvement ratios over the deterministic counterparts. Holdout: 75% training set-25% testing set.

We notice that all the considered robust formulations outperform the corresponding determin-

istic models. In 6 out of 12 datasets the best results are achieved by the box robust formulation ($p = \infty$). Since box uncertainty sets are the widest around data points, this implies that the proposed formulations benefit from a more conservative approach when treating uncertainties. The computation of the robust improvement ratio over the deterministic counterpart confirms that robust methods provide superior accuracy when the uncertainty is handled in the classification process. Extensive results on the improvement ratio are reported in Table B.22 in Appendix B.

For the sake of completeness, we explore in details the performance of the proposed models when classifying datasets “Parkinson” and “Breast Cancer Diagnostic”. First of all, we discuss the results of the deterministic approach, with respect to both data transformation and kernel function. The out-of-sample testing errors for the holdout 75%-25% are depicted in Figure 5, while detailed results are reported in Table B.7 in Appendix B. We note that the worst performances occur when no data transformations are applied. Conversely, min-max normalization and standardization provide good and comparable results. Similar conclusions can be drawn for holdouts 50%-50% and 25%-75% (see Tables B.8-B.9 in Appendix B).

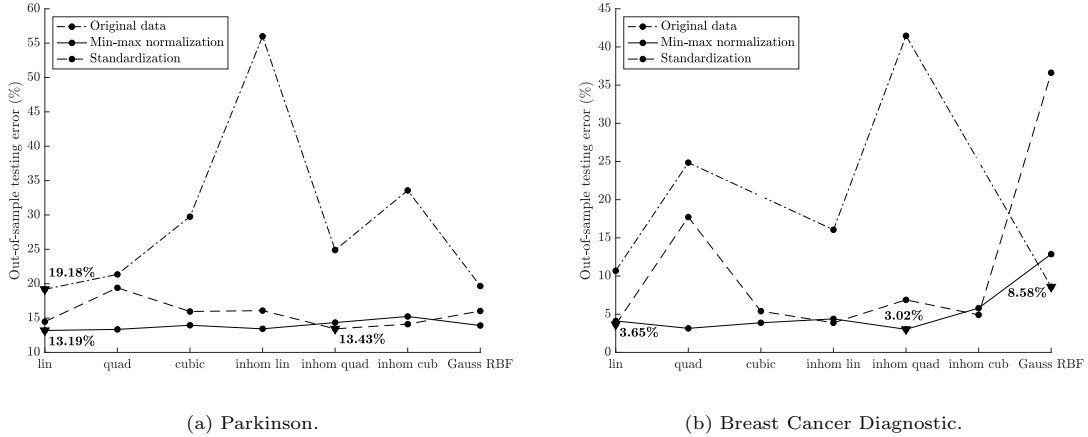
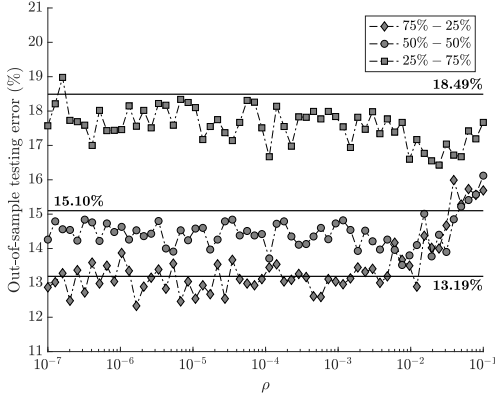


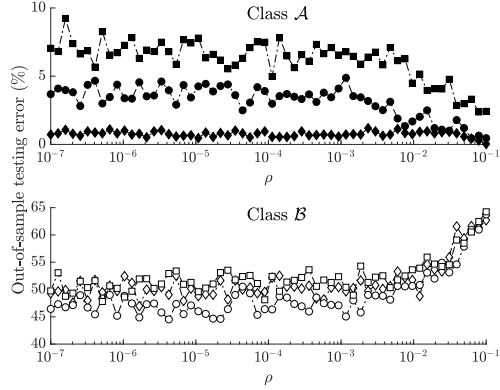
Figure 5: Out-of-sample testing error of the deterministic formulation applied to the datasets “Parkinson” and “Breast Cancer Diagnostic”. Each triangle represents the lowest error for the corresponding data transformation technique. Holdout: 75% training set-25% testing set.

In order to evaluate the performance of the robust model, we consider 60 logarithmically spaced values of ρ between 10^{-7} and 10^{-1} . The results are depicted in Figure 6. We notice that the increase of the value of β leads to better performances when considering the overall out-of-sample testing error (see Figures 6a, 6c), since more data points in the training set are available as input of the optimization model. In addition, when perturbations are included in the model, the performances improve with respect to the deterministic case. Indeed, the great majority of the points lies below the corresponding horizontal line, representing the out-of-sample testing error of the deterministic classifier. Interestingly, the increase of the uncertainty impacts differently on the two classes (see Figures 6b, 6d). For instance, the “Breast Cancer Diagnostic” dataset is not able to bear high levels of uncertainty ($\rho > 10^{-3}$) since all data points of class \mathcal{A} , representing patients with a malignant tumor, are misclassified. On the other hand, all observations in class \mathcal{B} (patients with a benign tumor) are assigned to the correct category. From a practical perspective, given that classifying people with a malignant tumor as people with a benign tumor is worse than the opposite, robust

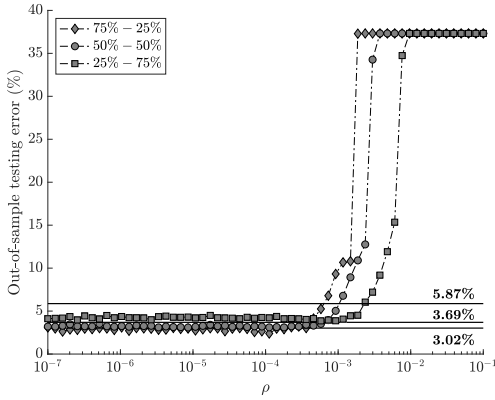
models with low degree of perturbation should be considered in this case.



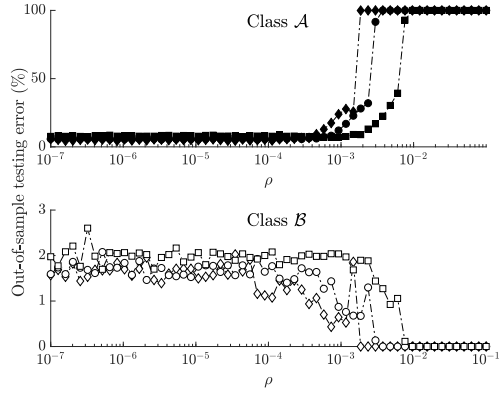
(a) Overall results (Parkinson).



(b) Results divided by class. (Parkinson).



(c) Overall results. (Breast Cancer Diagnostic).



(d) Results divided by class. (Breast Cancer Diagnostic).

Figure 6: Out-of-sample testing error of the robust formulation applied to the datasets “Parkinson” and “Breast Cancer Diagnostic”. Overall results are on the left, with the performance of the deterministic classifier depicted as horizontal line for each holdout. Results divided by class are on the right. The values of ρ are in logarithmic scale.

In Table 4 we report a comparison between the best results of Table 3 and the out-of-sample testing errors provided by *scikit-learn*, a popular ML library implemented in Python (Pedregosa et al. (2011)). We tested the seven different kernels, reporting in column 5 the best choice in terms of lowest out-of-sample testing error. From column 6, it can be noted that in 8 out of 10 datasets the formulation proposed in this study outperforms the one implemented in the *scikit-learn* library.

In addition, we compare the performance of our models with the results reported in Faccini et al. (2022) and Bertsimas et al. (2019). As shown in Table 5, in 6 out of 10 datasets the results of our deterministic classifiers outperform the other methods. Consequently, the linear approaches benefit from a generalization towards nonlinear classifier. Moreover, within the same 6 datasets, our robust formulation leads to even better accuracy.

To assess the good performance of the proposed approach over the two other methods, we applied the Friedman test and the Holm test (Demšar (2006)). First of all, we computed the average rank R_j , $j = 1, 2, 3$, for each of the three methods on the basis of the out-of-sample testing error (see columns 2 and 6 in Table 6). Then, the Friedman test with Iman-Davenport correction is applied to verify whether such ranks are statistically similar (null hypothesis). The statistic F_F

Dataset	Data transformation	Table 3		Scikit-learn library	
		Best kernel	Result	Best kernel	Result
Arrhythmia	–	Gaussian RBF	19.12% ± 0.08	Gaussian RBF	19.48% ± 0.07
Parkinson	Min-max normalization	Hom. linear	12.37% ± 0.03	Inhom. cubic	9.41% ± 0.04
Heart Disease	Standardization	Inhom. linear	16.36% ± 0.04	Inhom. linear	16.63% ± 0.04
Dermatology	–	Inhom. quadratic	0.55% ± 0.01	Inhom. linear	0.11% ± 0.01
Climate Model Crashes	–	Hom. linear	4.34% ± 0.01	Inhom. linear	4.78% ± 0.01
Breast Cancer Diagnostic	Min-max normalization	Inhom. quadratic	2.39% ± 0.01	Hom. cubic	2.78% ± 0.01
Breast Cancer	Standardization	Hom. linear	2.97% ± 0.01	Gaussian RBF	3.04% ± 0.01
Blood Transfusion	Standardization	Inhom. cubic	20.55% ± 0.02	Inhom. cubic	21.65% ± 0.02
Mammographic Mass	Standardization	Inhom. quadratic	15.42% ± 0.02	Inhom. quadratic	16.05% ± 0.02
Qsar Biodegradation	Min-max normalization	Gaussian RBF	11.78% ± 0.01	Inhom. quadratic	12.57% ± 0.02

Table 4: Out-of-sample testing error comparison among best results of Table 3 and simulations from the scikit-learn library (Pedregosa et al. (2011)). The lowest out-of-sample testing error within a dataset is highlighted.

Dataset	Deterministic formulation			Robust formulation		
	Table 3	Faccini et al. (2022)	Bertsimas et al. (2019)	Table 3	Faccini et al. (2022)	Bertsimas et al. (2019)
Arrhythmia	<u>20.47%</u>	25.65%	43.08%	19.12%	23.00%	29.23%
Parkinson	13.19%	14.13%	14.36%	12.37%	13.00%	16.41%
Heart Disease	17.48%	16.68%	15.93%	16.36%	<u>16.20%</u>	16.61%
Dermatology	1.64%	<u>0.56%</u>	3.38%	0.55%	0.13%	1.13%
Climate Model Crashes	5.01%	<u>4.99%</u>	5.00%	4.34%	4.34%	4.07%
Breast Cancer Diagnostic	<u>3.02%</u>	4.89%	6.49%	2.39%	3.89%	4.04%
Breast Cancer	<u>3.17%</u>	3.49%	5.00%	2.97%	3.12%	4.26%
Blood Transfusion	<u>20.72%</u>	23.49%	23.62%	20.55%	22.55%	23.62%
Mammographic Mass	<u>15.71%</u>	–	18.07%	15.42%	–	19.28%
Qsar Biodegradation	12.88%	–	<u>12.51%</u>	11.78%	–	12.42%

Table 5: Out-of-sample testing error comparison among deterministic and robust results of Table 3, data from Faccini et al. (2022) and Bertsimas et al. (2019). For each approach and dataset, the best result is underlined. The lowest out-of-sample testing error within a dataset is in bold.

associated with the test is given by:

$$F_F = \frac{(N_d - 1)\chi_F^2}{N_d(N_m - 1) - \chi_F^2}, \quad \text{with} \quad \chi_F^2 = \frac{12N_d}{N_m(N_m + 1)} \left[\sum_{j=1}^{N_m} R_j^2 - \frac{N_m(N_m + 1)^2}{4} \right],$$

where $N_d = 8$ is the number of datasets (we excluded “Mammographic Mass” and “Qsar Biodegradation” since they were not considered in Faccini et al. (2022)) and $N_m = 3$ is the number of methodologies. Under the null hypothesis, F_F is distributed according to the F -distribution with $N_m - 1$ and $(N_m - 1)(N_d - 1)$ degrees of freedom. In our case, the p -values associated with the Friedman test are 0.085 and 0.014 for the deterministic and robust approach, respectively. This implies that the null hypothesis of equal ranks is rejected with a significance level lower than $\alpha_D = 10\%$ and $\alpha_R = 5\%$, respectively. Since such hypothesis does not hold, we performed pairwise comparisons between the classifier with the highest rank R^* and those remaining. To this extent, we considered the Holm test (Demšar (2006)) whose statistic z_j for comparing the best classifier with the j -th one is computed as:

$$z_j = (R^* - R_j) \sqrt{\frac{6N_d}{N_m(N_m + 1)}}.$$

Under the null hypothesis of outperformance of the best method over the others, the test statistic is distributed as a standard normal distribution. The results of the Holm test are presented in Table 6. The null hypothesis is rejected when the p -value of the test is below the significance thresholds of columns 4 and 8. It can be seen that the proposed model achieves the highest rank in both the

deterministic and robust formulation, outperforming the standard linear SVM approach presented in Bertsimas et al. (2019). On the other hand, there are no statistically significant differences between our proposal and the robust method devised in Faccini et al. (2022), even if in most cases the results confirm the good performance of the proposed methodology (see Table 5).

Method	Deterministic				Robust			
	Mean rank	p -value	$\alpha_D/(j-1)$	Action	Mean rank	p -value	$\alpha_R/(j-1)$	Action
Table 3	1.625	-	-	-	1.438	-	-	-
Faccini et al. (2022)	1.750	0.803	0.100	Not reject	1.813	0.453	0.050	Not reject
Bertsimas et al. (2019)	2.625	0.046	0.050	Reject	2.750	0.009	0.025	Reject

Table 6: Holm test for pairwise comparison, with $\alpha_D = 0.1$, $\alpha_R = 0.05$ and $j = 2, 3$.

From Table 3 it can be noticed that the choice of the best data transformation method strongly depends on the dataset. In order to guide the final user among the three possible techniques, we report in Table B.23 in Appendix B summary statistics on the 10 datasets deployed for binary classification task. Specifically, for each feature we compute the mean and the corresponding coefficient of variation, defined as the ratio between the standard deviation and the mean. In Table B.23 we list the minimum and the maximum values of the two considered indices for each dataset, along with the corresponding best data transformation. We argue that, whenever the values of the observations are close, the best approach is to classify the original data without any transformation (see datasets “Arrhythmia”, “Dermatology” and “Climate Model Crashes”). In the extreme case of constant features, pre-processing techniques of data transformation cannot be applied (see dataset “Arrhythmia”). On the other hand, the min-max normalization is a suitable choice when the order of magnitude across the features varies a lot. For instance, in datasets “Parkinson” and “Breast Cancer Diagnostic” there are 7 and 5 orders of magnitude of difference between the minimum and the maximum value of the mean of the features, respectively. Finally, standardization is an appropriate technique in all other cases, where no significant differences occur among the orders of magnitude of the features (see datasets “Heart Disease”, “Breast Cancer”, “Blood Transfusion” and “Mammographic Mass”).

Finally, numerical results show that the computational time is significantly high for datasets with a large number of observations, especially when considering 75% of the instances as training set (see Table B.7 in Appendix B). The performing speed benefits from a reduction of β , even if at the cost of worsening the accuracy. Nevertheless, when datasets are equally split in training and testing set, the out-of-sample testing error does not increase significantly if compared to the holdout 75%-25% (see Table B.8). A similar conclusion can be drawn for the robust model (see Tables B.13-B.16). Conversely, from the time complexity analysis, it should be noticed that the number N_{\max} of sub-intervals chosen to solve problem (8) and its variants impacts on the overall computational time especially when the number of observations is not significantly high. Therefore, the final user should properly choose the values of β and N_{\max} to guarantee high accuracy in a reasonable time.

7. Conclusions

In this paper, we have proposed novel optimization models for solving binary and multiclass classification tasks through SVM. From a methodological perspective, we have extended the tech-

niques presented in Liu & Potra (2009); Faccini et al. (2022) to the nonlinear context through the introduction of kernel functions. Data are mapped from the input space to a higher-dimensional space where a first classification is performed. The optimal classifier is then constructed as the solution of a linear search procedure aiming to minimize the overall misclassification error.

Motivated by the uncertain nature of real-world data, we have adopted a RO approach by constructing around each input data a bounded-by- ℓ_p -norm uncertainty set, with $p \in [1, \infty]$. Perturbation propagates from the input space to the feature space through the kernel function. To this extent, we have derived closed-form expressions for the uncertainty sets bounds in the feature space, extending the results present in the literature. Thanks to this, we have derived the robust counterpart of the deterministic models in the case of nonlinear classifiers. To enhance generalization, in all the proposed formulations we have considered a ℓ_q -norm with $q \in [1, \infty]$ as measure of the SVM-margin. Since the resulting problem turns to be nonlinear, we have proved that in specific cases it can be reduced as a LP or a SOCP problem, with clear advantages in terms of computational efficiency.

The proposed models have been tested on real-world datasets, considering different combinations of data transformations and kernel functions. The results show that our formulations outperform other linear and nonlinear SVM approaches in most cases, even in the deterministic framework. This has been confirmed by classical statistical tests deployed to compare the performance of ML techniques. Overall, the models benefit from including uncertainty in the training process. The accuracy is clearly affected by the choice of the kernel function and of the data transformation before training. Therefore, we have provided insights to guide the final user in choosing the best configuration.

Regarding future advancements, various streams of research can originate from this work. First of all, extend the approach to handle uncertainties in the labels of input data. This should increase the generalization capability of the models. Additionally, in this work we have followed the classical RO approach of including uncertainty during the training phase (see, for instance, Bertsimas et al. (2019)). It should be noteworthy to consider perturbations both in the training and in the testing sets. However, this choice increases the complexity of the models and novel measures to quantify the accuracy have to be devised, since it is not obvious how to classify an entire uncertainty set in one class or another as opposed to the case of single data point. The main limitation of the current proposal is the complexity of the two-steps procedure, leading to a time-consuming process. Further techniques should be used to speed up the approach, especially in the phase of tuning parameters (see, for example, the Bayesian optimization in Snoek et al. (2012)). Finally, different methodologies should be applied to further robustify the models. For instance, Chance-Constrained Programming and Distributionally Robust Optimization with ambiguity sets defined by moments, phi-divergences or Wasserstein distance merit further research too.

Acknowledgements

This work has been supported by “ULTRA OPTYMAL - Urban Logistics and sustainable TRAnspOrtation: OPTimization under uncertainTY and MACHine Learning”, a PRIN2020 project funded by the Italian University and Research Ministry (grant number 20207C8T9M).

This study was also carried out within the MOST - Sustainable Mobility National Research Center and received funding from the European Union Next-GenerationEU (PIANO NAZIONALE DI RIPRESA E RESILIENZA (PNRR) – MISSIONE 4 COMPONENTE 2, INVESTIMENTO 1.4 – D.D. 1033 17/06/2022, CN00000023), Spoke 5 “Light Vehicle and Active Mobility”. This manuscript reflects only the authors’ views and opinions, neither the European Union nor the European Commission can be considered responsible for them.

References

References

- Ben-Tal, A., Bhadra, S., Bhattacharyya, C., & Nemirovski, A. (2012). Efficient methods for robust classification under uncertainty in kernel matrices. *Journal of Machine Learning Research*, *13*, 2923–54.
- Ben-Tal, A., El Ghaoui, L., & Nemirovski, A. (2009). Robust optimization. Princeton University Press.
- Bengio, Y., Lodi, A., & Prouvost, A. (2021). Machine learning for combinatorial optimization: A methodological tour d’horizon. *European Journal of Operational Research*, *290*, 405–21.
- Bennett, K. P., & Mangasarian, O. L. (1992). Robust linear programming discrimination of two linearly inseparable sets. *Optimization Methods & Software*, *1*, 23–34.
- Bertsimas, D., Brown, D. B., & Caramanis, C. (2011). Theory and applications of robust optimization. *SIAM review*, *53*, 464–501.
- Bertsimas, D., Dunn, J., Pawlowski, C., & Zhuo, Y. D. (2019). Robust classification. *INFORMS Journal of Optimization*, *1*, 2–34.
- Bhadra, S., Bhattacharya, S., Bhattacharyya, C., & Ben-Tal, A. (2010). Robust formulations for handling uncertainty in kernel matrices. *Proceedings for the 27th International Conference on Machine Learning*, (pp. 71–8).
- Bhattacharyya, C. (2004). Robust classification of noisy data using second order cone programming approach. In *International Conference on Intelligent Sensing and Information Processing, 2004* (pp. 433–8).
- Bi, J., & Zhang, T. (2005). Support vector classification with input data uncertainty. In *Advances in neural information processing systems* (pp. 161–8).
- Blanco, V., Puerto, J., & Rodríguez-Chía, A. M. (2020). On lp-support vector machines and multidimensional kernels. *Journal of Machine Learning Research*, *21*, 1–29.
- Boser, B. E., Guyon, I., & Vapnik, V. N. (1992). A training algorithm for optimal margin classifiers. *Proceedings of the Fifth Annual Workshop of Computational Learning Theory*, *5*, 144–52.

- Cervantes, J., Garcia-Lamont, F., Rodríguez-Mazahua, L., & Lopez, A. (2020). A comprehensive survey on support vector machine classification: Applications, challenges and trends. *Neurocomputing*, *408*, 189–215.
- Chen, T. Y., Tse, T. H., & Yu, Y.-T. (2001). Proportional sampling strategy: a compendium and some insights. *The Journal of Systems and Software*, *58*, 65–81.
- Chen, Z.-Y., Fan, Z.-P., & Sun, M. (2012). A hierarchical multiple kernel support vector machine for customer churn prediction using longitudinal behavioral data. *European Journal of Operational Research*, *223*, 461–72.
- Cortes, C., & Vapnik, V. N. (1995). Support-vector networks. *Machine Learning*, *20*, 273–97.
- De Bock, K. W., Coussement, K., Caigny, A. D., Słowiński, R., Baesens, B., Boute, R. N., Choi, T.-M., Delen, D., Kraus, M., Lessmann, S., Maldonado, S., Martens, D., Óskarsdóttir, M., Vairetti, C., Verbeke, W., & Weber, R. (2023). Explainable ai for operational research: A defining framework, methods, applications, and a research agenda. *European Journal of Operational Research*, *in press*.
- De Leone, R., Maggioni, F., & Spinelli, A. (2023). A robust twin parametric margin support vector machine for multiclass classification. URL: <https://arxiv.org/abs/2306.06213>.
- De Leone, R., Maggioni, F., & Spinelli, A. (2024). A multiclass robust twin parametric margin support vector machine with an application to vehicles emissions. In G. Nicosia, V. Ojha, E. La Malfa, G. La Malfa, P. M. Pardalos, & R. Umeton (Eds.), *Machine Learning, Optimization, and Data Science* (pp. 299–310). Cham: Springer Nature Switzerland volume 14506 of *Lecture Notes in Computer Science*. doi:https://doi.org/10.1007/978-3-031-53966-4_22.
- Demšar, J. (2006). Statistical comparisons of classifiers over multiple data sets. *Journal of Machine Learning Research*, *7*, 1–30.
- Ding, S., & Hua, X. (2014). Recursive least squares projection twin support vector machines for nonlinear classification. *Neurocomputing*, *130*, 3–9. Track on Intelligent Computing and Applications Complex Learning in Connectionist Networks.
- Ding, S., Zhao, X., Zhang, J., Zhang, X., & Xue, Y. (2019). A review on multi-class twsvm. *Artificial Intelligence Review*, *52*, 775–801.
- Doumpos, M., Zopounidis, C., Gounopoulos, D., Platanakis, E., & Zhang, W. (2023). Operational research and artificial intelligence methods in banking. *European Journal of Operational Research*, *306*, 1–16.
- Du, S.-W., Zhang, M.-C., Chen, P., Sun, H.-F., Chen, W.-J., & Shao, Y.-H. (2021). A multiclass nonparallel parametric-margin support vector machine. *Information*, *12*, 515–33.
- El Ghaoui, L., Lanckriet, G. R. G., Natsoulis, G. et al. (2003). Robust classification with interval data. In *Computer Science Division, University of California Berkeley*.

- Faccini, D., Maggioni, F., & Potra, F. A. (2022). Robust and distributionally robust optimization models for linear support vector machine. *Computers and Operations Research*, *147*, 105930.
- Fan, N., Sadeghi, E., & Pardalos, P. M. (2014). Robust support vector machines with polyhedral uncertainty of the input data. In *Learning and Intelligent Optimization. International Conference on Learning and Intelligent Optimization* (pp. 291–305). Springer-Verlag.
- Fung, G., Mangasarian, O. L., & Shavlik, J. W. (2002). Knowledge-based support vector machine classifiers. In *NIPS* (pp. 521–8).
- Gambella, C., Ghaddar, B., & Naoum-Sawaya, J. (2021). Optimization problems for machine learning: A survey. *European Journal of Operational Research*, *290*, 807–28.
- Grant, M., & Boyd, S. (2008). Graph implementations for nonsmooth convex programs. In V. Blondel, S. Boyd, & H. Kimura (Eds.), *Recent Advances in Learning and Control Lecture Notes in Control and Information Sciences* (pp. 95–110). Springer-Verlag Limited. http://stanford.edu/~boyd/graph_dcp.html.
- Grant, M., & Boyd, S. (2014). CVX: Matlab software for disciplined convex programming, version 2.1. <http://cvxr.com/cvx>.
- Gunnarsson, B. R., vanden Broucke, S., Baesens, B., Óskarsdóttir, M., & Lemahieu, W. (2021). Deep learning for credit scoring: Do or don't? *European Journal of Operational Research*, *295*, 292–305.
- Han, J., Kamber, M., & Pei, J. (2011). *Data mining: concepts and techniques - 3rd edition*. Morgan Kaufmann.
- Hao, P.-Y. (2010). New support vector algorithms with parametric insensitive/margin model. *Neural networks : the official journal of the International Neural Network Society*, *23*, 60–73.
- Jayadeva, Khemchandani, R., & Chandra, S. (2007). Twin support vector machines for pattern classification. *IEEE Transactions on Pattern Analysis and Machine Intelligence*, *29*, 905–10.
- Jiang, J., & Peng, S. (2024). Mathematical programs with distributionally robust chance constraints: Statistical robustness, discretization and reformulation. *European Journal of Operational Research*, *313*, 616–27.
- Jiménez-Cordero, A., Morales, J. M., & Pineda, S. (2021). A novel embedded min-max approach for feature selection in nonlinear support vector machine classification. *European Journal of Operational Research*, *293*, 24–35.
- Ju, X., & Tian, Y. (2012). Knowledge-based support vector machine classifiers via nearest points. *Procedia Computer Science*, *9*, 1240–8.
- Kelly, M., Longjohn, R., & Nottingham, K. (2023). UCI machine learning repository. URL: <http://archive.ics.uci.edu/ml>.

- Ketkov, S. S. (2024). A study of distributionally robust mixed-integer programming with wasserstein metric: on the value of incomplete data. *European Journal of Operational Research*, *313*, 602–15.
- Khanjani-Shiraz, R., Babapour-Azar, A., Hosseini-Nodeh, Z., & Pardalos, P. M. (2023). Distributionally robust joint chance-constrained support vector machines. *Optimization Letters*, *17*, 299–332.
- Kim, J.-H. (2009). Estimating classification error rate: Repeated cross-validation, repeated hold-out and bootstrap. *Computational Statistics and Data Analysis*, *53*, 3735–45.
- Labbé, M., Martínez-Merino, L. I., & Rodríguez-Chía, A. M. (2019). Mixed integer linear programming for feature selection in support vector machine. *Discrete Applied Mathematics*, *261*, 276–304.
- Lanckriet, G. R. G., Ghaoui, L. E., Bhattacharyya, C., & Jordan, M. I. (2002). A robust minimax approach to classification. *Journal of Machine Learning Research*, *3*, 555–82.
- Lee, Y.-J., Mangasarian, O. L., & Wolberg, W. H. (2000). Breast cancer survival and chemotherapy: a support vector machine analysis. *Discrete mathematical problems with medical applications*, *55*, 1–10.
- Li, H., Liang, Y., & Xu, Q. (2009). Support vector machines and its applications in chemistry. *Chemometrics and Intelligent Laboratory Systems*, *95*, 188–98.
- Liu, X., & Potra, F. A. (2009). Pattern separation and prediction via linear and semidefinite programming. *Studies in Informatics and Control*, *18*, 71–82.
- López, J., Maldonado, S., & Carrasco, M. (2017). A robust formulation for twin multiclass support vector machine. *Applied Intelligence*, *47*, 1031–43.
- López, J., Maldonado, S., & Carrasco, M. (2018). Double regularization methods for robust feature selection and svm classification via dc programming. *Information Sciences*, *429*, 377–89.
- López, J., Maldonado, S., & Carrasco, M. (2019). Robust nonparallel support vector machines via second-order cone programming. *Neurocomputing*, *364*, 227–38.
- Luo, J., Yan, X., & Tian, Y. (2020). Unsupervised quadratic surface support vector machine with application to credit risk assessment. *European Journal of Operational Research*, *280*, 1008–17.
- Maggioni, F., Faccini, D., Gheza, F., Manelli, F., & Bonetti, G. (2023). Machine learning based classification models for covid-19 patients. In R. Aringhieri, F. Maggioni, E. Lanzarone, M. Reuter-Oppermann, G. Righini, & M. T. Vespucci (Eds.), *Operations Research for Health Care in Red Zone* (pp. 35–46). Cham: Springer International Publishing.
- Maggioni, F., Potra, F. A., Bertocchi, M., & Allevi, E. (2009). Stochastic second-order cone programming in mobile ad hoc networks. *Journal of Optimization Theory and Applications*, *143*, 309–28.

- Maggioni, F., & Spinelli, A. (2024). A robust nonlinear support vector machine approach for vehicles smog rating classification. In M. Bruglieri, P. Festa, G. Macrina, & O. Pisacane (Eds.), *Optimization in Green Sustainability and Ecological Transition* AIRO Springer Series. Springer Cham. doi:https://doi.org/10.1007/978-3-031-47686-0_19.
- Maldonado, S., López, J., & Carrasco, M. (2022). The cobb-douglas learning machine. *Pattern Recognition*, *128*, 108701.
- Maldonado, S., López, J., & Vairetti, C. (2020). Profit-based churn prediction based on minimax probability machines. *European Journal of Operational Research*, *284*, 273–84.
- Mangasarian, O. L. (1998). Generalized support vector machines. In *Advances in Large Margin Classifiers* (pp. 135–46). MIT Press.
- Marcelli, E., & De Leone, R. (2020). Multi-kernel covariance terms in multi-output support vector machines. In G. Nicosia, V. Ojha, E. La Malfa, G. Jansen, V. Sciacca, P. Pardalos, G. Giuffrida, & R. Umeton (Eds.), *Machine Learning, Optimization, and Data Science* (pp. 1–11). Cham: Springer International Publishing.
- Mi, C., Wang, J., Mi, W., Huang, Y., Zhang, Z., Yang, Y., Jiang, J., & Octavian, P. (2019). Research on regional clustering and two-stage svm method for container truck recognition. *Discrete and Continuous Dynamical Systems - S*, *12*, 1117–33.
- MOSEK ApS (2019). *The MOSEK optimization toolbox for MATLAB manual. Version 9.1*. URL: <http://docs.mosek.com/9.1/toolbox/index.html>.
- Pedregosa, F., Varoquaux, G., Gramfort, A., Michel, V., Thirion, B., Grisel, O., Blondel, M., Prettenhofer, P., Weiss, R., Dubourg, V., Vanderplas, J., Passos, A., Cournapeau, D., Brucher, M., Perrot, M., & Duchesnay, E. (2011). Scikit-learn: Machine learning in Python. *Journal of Machine Learning Research*, *12*, 2825–30.
- Peng, X. (2011). Tpm SVM: A novel twin parametric-margin support vector machine for pattern recognition. *Pattern Recognition*, *44*, 2678–92.
- Peng, X., & Xu, D. (2013). Robust minimum class variance twin support vector machine classifier. *Neural Computing and Applications*, *22*, 999–1011.
- Piccialli, V., & Sciadrone, M. (2018). Nonlinear optimization and support vector machines. *4OR - A Quarterly Journal of Operations Research*, *16*, 111–49.
- Qi, Z., Tian, Y., & Shi, Y. (2013). Robust twin support vector machine for pattern classification. *Pattern Recognition*, *46*, 305–16.
- Raeesi, R., Sahebjamnia, N., & Mansouri, S. A. (2023). The synergistic effect of operational research and big data analytics in greening container terminal operations: A review and future directions. *European Journal of Operational Research*, *310*, 943–73.
- Rudin, W. (1987). *Real and complex analysis*. McGraw-Hill.

- Schölkopf, B., Smola, A., Williamson, R. C., & Bartlett, P. L. (2000). New support vector algorithms. *Neural Computation*, *12*, 1207–45.
- Schölkopf, B., & Smola, A. J. (2001). *Learning with Kernels: Support Vector Machines, regularization, optimization, and beyond*. MIT press.
- Singla, M., Ghosh, D., & Shukla, K. K. (2020). A survey of robust optimization based machine learning with special reference to support vector machines. *International Journal of Machine Learning and Cybernetics*, *11*, 1359–85.
- Snoek, J., Larochelle, H., & Adams, R. P. (2012). Practical bayesian optimization of machine learning algorithms. In F. Pereira, C. Burges, L. Bottou, & K. Weinberger (Eds.), *Advances in Neural Information Processing Systems*. Curran Associates, Inc. volume 25.
- Szelag, M., & Słowiński, R. (2023). Explaining and predicting customer churn by monotonic rules induced from ordinal data. *European Journal of Operational Research*, *in press*.
- Tanveer, M., Rajani, T., Rastogi, R., & Shao, Y. (2022). Comprehensive review on twin support vector machines. *Annals of Operations Research*, (pp. 1–46).
- Tay, F. E., & Cao, L. (2001). Application of support vector machines in financial time series forecasting. *Omega*, *29*, 309–17.
- Trafalis, T. B., & Alwazzi, S. A. (2010). Support vector machine classification with noisy data: a second order cone programming approach. *International Journal of General Systems*, *39*, 757–81.
- Trafalis, T. B., & Gilbert, R. C. (2006). Robust classification and regression using support vector machines. *European Journal of Operational Research*, *173*, 893–909.
- Vapnik, V. N. (1995). *The nature of statistical learning theory*. Springer-Verlag.
- Vapnik, V. N., & Chervonenkis, A. Y. (1974). *Theory of Pattern Recognition*. Nauka, Moscow.
- Wang, H., Zheng, B., Yoon, S. W., & Ko, H. S. (2018a). A support vector machine-based ensemble algorithm for breast cancer diagnosis. *European Journal of Operational Research*, *267*, 687–99.
- Wang, X., Fan, N., & Pardalos, P. M. (2018b). Robust chance-constrained support vector machines with second-order moment information. *Annals of Operations Research*, *263*, 45–68.
- Wang, X., & Pardalos, P. M. (2014). A survey of support vector machines with uncertainties. *Annals of Data Science*, *1*, 293–309.
- Wei, Z., Hao, J.-K., Ren, J., & Glover, F. (2023). Responsive strategic oscillation for solving the disjunctively constrained knapsack problem. *European Journal of Operational Research*, *309*, 993–1009.
- Xu, H., Caramanis, C., & Mannor, S. (2009). Robustness and regularization of support vector machines. *Journal of Machine Learning Research*, *10*, 1485–510.

- Yajima, Y. (2005). Linear programming approaches for multicategory support vector machines. *European Journal of Operational Research*, 162, 514–31.
- Yao, X., Crook, J., & Andreeva, G. (2017). Enhancing two-stage modelling methodology for loss given default with support vector machines. *European Journal of Operational Research*, 263, 679–89.

Appendix A. Supplementary proofs

We first recall a lemma that will be useful to prove Propositions 1-2.

Lemma 1 (Inequalities in ℓ_p -norm). Let x be a vector in \mathbb{R}^n . If $1 \leq p \leq q \leq \infty$, then:

$$\|x\|_q \leq \|x\|_p \leq n^{\frac{1}{p} - \frac{1}{q}} \|x\|_q. \quad (\text{A.1})$$

Proof. We consider the two inequalities separately, starting from $\|x\|_q \leq \|x\|_p$. First of all, if $x = 0$, then the inequality is obviously true. Otherwise, let $y \in \mathbb{R}^n$ such that $y_i := |x_i| / \|x\|_q$ for $i = 1, \dots, n$. Therefore, $0 \leq y_i \leq 1$. Indeed:

$$\|x\|_q^q = \sum_{i=1}^n |x_i|^q \geq |x_i|^q,$$

for all $i = 1, \dots, n$ and thus $|x_i| / \|x\|_q \leq 1$. The hypothesis $p \leq q$ and the decreasing property of the exponential function with basis lower than one imply that:

$$y_i^p \geq y_i^q, \quad i = 1, \dots, n.$$

By summing we have:

$$\|y\|_p \geq \|y\|_q.$$

Finally, by definition of y we derive that:

$$\frac{\|x\|_p}{\|x\|_q} \geq \frac{\|x\|_q}{\|x\|_q} = 1,$$

from which the thesis follows.

On the other hand, to prove the second inequality we recall the Hölder inequality (see, for instance, Rudin (1987)). Let a and b be in \mathbb{R}^n . If r and r' are conjugate exponents, i.e. $\frac{1}{r} + \frac{1}{r'} = 1$, with $1 \leq r, r' \leq \infty$, then:

$$\|ab\|_1 \leq \|a\|_r \cdot \|b\|_{r'},$$

or, equivalently:

$$\sum_{i=1}^n |a_i| |b_i| \leq \left(\sum_{i=1}^n |a_i|^r \right)^{\frac{1}{r}} \cdot \left(\sum_{i=1}^n |b_i|^{r'} \right)^{\frac{1}{r'}}. \quad (\text{A.2})$$

First of all, we rewrite the ℓ_p -norm of x as:

$$\|x\|_p^p = \sum_{i=1}^n |x_i|^p = \sum_{i=1}^n |x_i|^p \cdot 1.$$

In the Hölder inequality (A.2), let $a = x$ and $b = e$ and consider as conjugate exponents $r = \frac{q}{p}$ and $r' = \frac{q}{q-p}$. Both r and r' are greater than or equal to 1 because, by hypothesis, $p \leq q$.

Consequently, we can bound the ℓ_p -norm of x by:

$$\|x\|_p^p \leq \left(\sum_{i=1}^n (|x_i|^p)^{\frac{q}{p}} \right)^{\frac{p}{q}} \cdot \left(\sum_{i=1}^n 1^{\frac{q}{q-p}} \right)^{1-\frac{p}{q}} = \left(\sum_{i=1}^n |x_i|^q \right)^{\frac{p}{q}} n^{1-\frac{p}{q}} = \|x\|_q^p n^{1-\frac{p}{q}}.$$

Finally, the thesis follows by taking the p -th root of both sides of the inequality. \square

A graphical representation of inequality (A.1) is depicted in Figure A.7.

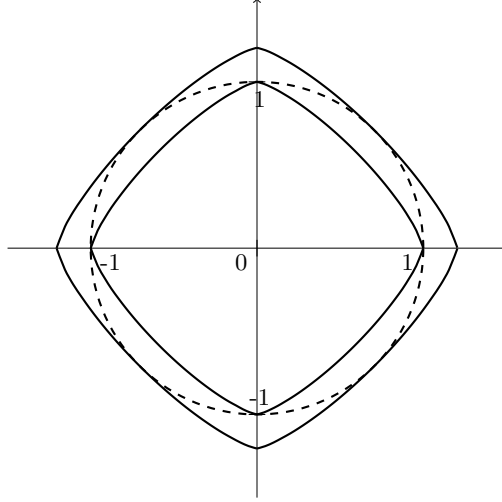


Figure A.7: Graphical representation of Lemma 1 in the case of $p = 1.3$, $q = 2$, $n = 2$. The dashed ℓ_2 unit ball lies between the $\ell_{1.3}$ unit ball and the $\ell_{1.3}$ ball with radius $2^{\frac{1}{1.3}-\frac{1}{2}} \approx 1.205$.

As special cases, Lemma 1 implies that, whenever $1 \leq p \leq 2$, then:

$$\|x\|_2 \leq \|x\|_p. \quad (\text{A.3})$$

Conversely, if $p > 2$, then:

$$\|x\|_2 \leq n^{\frac{p-2}{2p}} \|x\|_p. \quad (\text{A.4})$$

Thus, combining these results, we can write:

$$\|x\|_2 \leq C \|x\|_p,$$

with:

$$C = C(n, p) = \begin{cases} 1, & 1 \leq p \leq 2 \\ n^{\frac{p-2}{2p}}, & p > 2. \end{cases} \quad (\text{A.5})$$

Proof of Proposition 1

Proof. The \mathcal{H} -norm of the vector of perturbation $\zeta^{(i)}$ in the feature space can be expanded as:

$$\begin{aligned}
\|\zeta^{(i)}\|_{\mathcal{H}}^2 &= \|\phi(x) - \phi(x^{(i)})\|_{\mathcal{H}}^2 \\
&= \|\phi(x^{(i)} + \sigma^{(i)}) - \phi(x^{(i)})\|_{\mathcal{H}}^2 \\
&= \langle \phi(x^{(i)} + \sigma^{(i)}) - \phi(x^{(i)}), \phi(x^{(i)} + \sigma^{(i)}) - \phi(x^{(i)}) \rangle \\
&= \langle \phi(x^{(i)} + \sigma^{(i)}), \phi(x^{(i)} + \sigma^{(i)}) \rangle - 2\langle \phi(x^{(i)} + \sigma^{(i)}), \phi(x^{(i)}) \rangle + \langle \phi(x^{(i)}), \phi(x^{(i)}) \rangle \\
&= k(x^{(i)} + \sigma^{(i)}, x^{(i)} + \sigma^{(i)}) - 2k(x^{(i)} + \sigma^{(i)}, x^{(i)}) + k(x^{(i)}, x^{(i)}).
\end{aligned} \tag{A.6}$$

By definition of the inhomogeneous polynomial kernel of degree d , the last right-hand side of (A.6) becomes:

$$\begin{aligned}
\|\zeta^{(i)}\|_{\mathcal{H}}^2 &= \left(\|x^{(i)} + \sigma^{(i)}\|_2^2 + c \right)^d - 2(\langle x^{(i)} + \sigma^{(i)}, x^{(i)} \rangle + c)^d + \left(\|x^{(i)}\|_2^2 + c \right)^d \\
&= \left(\|x^{(i)}\|_2^2 + \|\sigma^{(i)}\|_2^2 + 2\langle \sigma^{(i)}, x^{(i)} \rangle + c \right)^d - 2\left(\|x^{(i)}\|_2^2 + \langle \sigma^{(i)}, x^{(i)} \rangle + c \right)^d + \left(\|x^{(i)}\|_2^2 + c \right)^d.
\end{aligned}$$

By applying the Cauchy-Schwarz inequality in \mathbb{R}^n to the terms containing the dot product, the previous expression simplifies further, leading to:

$$\begin{aligned}
\|\zeta^{(i)}\|_{\mathcal{H}}^2 &\leq \left(\|x^{(i)}\|_2^2 + \|\sigma^{(i)}\|_2^2 + 2\|\sigma^{(i)}\|_2 \|x^{(i)}\|_2 + c \right)^d - 2\left(\|x^{(i)}\|_2^2 + \|\sigma^{(i)}\|_2 \|x^{(i)}\|_2 + c \right)^d + \left(\|x^{(i)}\|_2^2 + c \right)^d \\
&= \left[\left(\|x^{(i)}\|_2 + \|\sigma^{(i)}\|_2 \right)^2 + c \right]^d - 2\left[\|x^{(i)}\|_2 \left(\|x^{(i)}\|_2 + \|\sigma^{(i)}\|_2 \right) + c \right]^d + \left(\|x^{(i)}\|_2^2 + c \right)^d.
\end{aligned}$$

Applying the binomial expansion to three d -th powers implies that:

$$\begin{aligned}
\|\zeta^{(i)}\|_{\mathcal{H}}^2 &\leq \sum_{k=0}^d \binom{d}{k} c^k \left(\|x^{(i)}\|_2 + \|\sigma^{(i)}\|_2 \right)^{2(d-k)} - 2 \sum_{k=0}^d \binom{d}{k} c^k \|x^{(i)}\|_2^{d-k} \left(\|x^{(i)}\|_2 + \|\sigma^{(i)}\|_2 \right)^{d-k} \\
&\quad + \sum_{k=0}^d \binom{d}{k} c^k \|x^{(i)}\|_2^{2(d-k)}.
\end{aligned}$$

We now split all the three sums by considering separately the cases when $k = 0$, $k = d$ and, then, all the intermediate cases. Firstly, let us call a_0 the addendum of the sum corresponding to

$k = 0$. Therefore:

$$\begin{aligned}
a_0 &= \left(\|x^{(i)}\|_2 + \|\sigma^{(i)}\|_2 \right)^{2d} - 2 \|x^{(i)}\|_2^d \left(\|x^{(i)}\|_2 + \|\sigma^{(i)}\|_2 \right)^d + \|x^{(i)}\|_2^{2d} \\
&= \left[\left(\|x^{(i)}\|_2 + \|\sigma^{(i)}\|_2 \right)^d - \|x^{(i)}\|_2^d \right]^2 \\
&= \left[\sum_{k=0}^d \binom{d}{k} \|x^{(i)}\|_2^{d-k} \|\sigma^{(i)}\|_2^k - \|x^{(i)}\|_2^d \right]^2 \\
&= \left[\sum_{k=1}^d \binom{d}{k} \|x^{(i)}\|_2^{d-k} \|\sigma^{(i)}\|_2^k + \|x^{(i)}\|_2^d - \|x^{(i)}\|_2^d \right]^2 = \left[\sum_{k=1}^d \binom{d}{k} \|x^{(i)}\|_2^{d-k} \|\sigma^{(i)}\|_2^k \right]^2.
\end{aligned}$$

We notice that a_0 is the only addendum of the sum that does not contain c . This implies that a_0 is related to the bound $\delta_{d,0}^{(i)}$ for the homogeneous polynomial kernel. Secondly, if $k = d$, we have no contribution because $c^d - 2c^d + c^d = 0$. Before considering the cases $k = 1, \dots, d-1$, we now investigate what happens when the degree d is equal to 1. Here, the index k of the sums goes from 0 to 1, and therefore, as seen before:

$$\|\zeta^{(i)}\|_{\mathcal{H}}^2 \leq (\delta_{\text{hom}}^{(i)})^2 = (C\eta^{(i)})^2.$$

Hence, when $d = 1$, then $\delta_{1,c}^{(i)} = C\eta^{(i)}$. Conversely, when $d > 1$, we have all the addenda between $k = 1$ and $k = d-1$. Thus, by combining all the three sums together we have:

$$\begin{aligned}
\|\zeta^{(i)}\|_{\mathcal{H}}^2 &\leq a_0 + \sum_{k=1}^{d-1} \binom{d}{k} c^k \left[\left(\|x^{(i)}\|_2 + \|\sigma^{(i)}\|_2 \right)^{2(d-k)} - 2 \|x^{(i)}\|_2^{d-k} \left(\|x^{(i)}\|_2 + \|\sigma^{(i)}\|_2 \right)^{d-k} + \|x^{(i)}\|_2^{2(d-k)} \right] \\
&= a_0 + \sum_{k=1}^{d-1} \binom{d}{k} c^k \left[\left(\|x^{(i)}\|_2 + \|\sigma^{(i)}\|_2 \right)^{d-k} - \|x^{(i)}\|_2^{d-k} \right]^2.
\end{aligned}$$

Again, by applying the binomial expansion to the $(d-k)$ -th power of $(\|x^{(i)}\|_2 + \|\sigma^{(i)}\|_2)$ and by splitting the sum, we are able to simplify the last term. Hence:

$$\begin{aligned}
\|\zeta^{(i)}\|_{\mathcal{H}}^2 &\leq a_0 + \sum_{k=1}^{d-1} \binom{d}{k} c^k \left[\sum_{j=0}^{d-k} \binom{d-k}{j} \|x^{(i)}\|_2^{d-k-j} \|\sigma^{(i)}\|_2^j - \|x^{(i)}\|_2^{d-k} \right]^2 \\
&= a_0 + \sum_{k=1}^{d-1} \binom{d}{k} c^k \left[\sum_{j=1}^{d-k} \binom{d-k}{j} \|x^{(i)}\|_2^{d-k-j} \|\sigma^{(i)}\|_2^j \right]^2.
\end{aligned}$$

Therefore, by taking the square root:

$$\|\zeta^{(i)}\|_{\mathcal{H}} \leq \sqrt{a_0 + \sum_{k=1}^{d-1} \binom{d}{k} c^k \left[\sum_{j=1}^{d-k} \binom{d-k}{j} \|x^{(i)}\|_2^{d-k-j} \|\sigma^{(i)}\|_2^j \right]^2}.$$

According to inequalities (A.3)–(A.4) and to hypothesis $\|\sigma^{(i)}\|_p \leq \eta^{(i)}$, we obtain that:

$$\|\sigma^{(i)}\|_2 \leq \begin{cases} \|\sigma^{(i)}\|_p \leq \eta^{(i)}, & 1 \leq p \leq 2 \\ n^{\frac{p-2}{2p}} \|\sigma^{(i)}\|_p \leq n^{\frac{p-2}{2p}} \eta^{(i)}, & p > 2. \end{cases}$$

Finally, whenever $1 \leq p \leq 2$, we have that:

$$a_0 \leq \left[\sum_{k=1}^d \binom{d}{k} \|x^{(i)}\|_2^{d-k} \|\sigma^{(i)}\|_p^k \right]^2 \leq \left[\sum_{k=1}^d \binom{d}{k} \|x^{(i)}\|_2^{d-k} (\eta^{(i)})^k \right]^2 = (\delta_{d,0}^{(i)})^2,$$

and the second addendum in the square root can be bounded by:

$$\sum_{k=1}^{d-1} \binom{d}{k} c^k \left[\sum_{j=1}^{d-k} \binom{d-k}{j} \|x^{(i)}\|_2^{d-k-j} (\eta^{(i)})^j \right]^2.$$

On the other hand, if $p > 2$, then:

$$a_0 \leq \left[\sum_{k=1}^d \binom{d}{k} \|x^{(i)}\|_2^{d-k} n^{\frac{k(p-2)}{2p}} \|\sigma^{(i)}\|_p^k \right]^2 \leq \left[\sum_{k=1}^d \binom{d}{k} \|x^{(i)}\|_2^{d-k} \left(n^{\frac{p-2}{2p}} \eta^{(i)} \right)^k \right]^2 = (\delta_{d,0}^{(i)})^2,$$

and similarly the second addendum in the square root is always less than or equal to:

$$\sum_{k=1}^{d-1} \binom{d}{k} c^k \left[\sum_{j=1}^{d-k} \binom{d-k}{j} \|x^{(i)}\|_2^{d-k-j} \left(n^{\frac{p-2}{2p}} \eta^{(i)} \right)^j \right]^2.$$

□

Proof of Proposition 2

Proof. For all x in \mathbb{R}^n , we have that $k(x, x) = 1$ and, thus, equation (A.6) reduces to:

$$\|\zeta^{(i)}\|_{\mathcal{H}}^2 = 1 - 2 \exp\left(-\frac{\|x^{(i)} + \sigma^{(i)} - x^{(i)}\|_2^2}{2\alpha^2}\right) + 1 = 2 - 2 \exp\left(-\frac{\|\sigma^{(i)}\|_2^2}{2\alpha^2}\right).$$

Therefore:

$$\|\zeta^{(i)}\|_{\mathcal{H}} = \sqrt{2 - 2 \exp\left(-\frac{\|\sigma^{(i)}\|_2^2}{2\alpha^2}\right)}.$$

The thesis follows by applying inequalities (A.3)–(A.4) and by considering the monotonicity of function $g(x) = -\exp(-x^2)$ when $x > 0$.

□

Proof of Corollary 1

- Proof.* a) If $q = 1$, model (18) can be rewritten as model (23) by introducing an auxiliary vector $s \in \mathbb{R}^m$ such that each component s_i is equal to $|u_i|$ and adding the constraints $s_i \geq 0$, $s_i \geq -u_i$ and $s_i \geq u_i$ for all $i = 1, \dots, m$.
- b) If $q = 2$, the quadratic term $\|u\|_2^2$ can be transformed from the objective function to the set of constraints by introducing auxiliary variables $r, t, v \in \mathbb{R}$ such that $t \geq \|u\|_2$, $r + v = 1$ and $r \geq \sqrt{t^2 + v^2}$ (Qi et al. (2013)). With the same reasoning at point a), model (18) reduces to model (24).
- c) If $q = \infty$, by introducing an auxiliary variable $s_\infty \geq 0$ equal to $\|u\|_\infty$, and adding the constraints $s_\infty \geq -u_i$ and $s_\infty \geq u_i$ for all $i = 1, \dots, m$, model (18) is equivalent to model (25) with the same reasoning at point a).

□

Appendix B. Supplementary results

Dataset	Data transformation	Kernel						
		Hom. linear	Hom. quadratic	Hom. cubic	Inhom. linear	Inhom. quadratic	Inhom. cubic	Gaussian RBF
Arrhythmia	–	21.94% ± 0.10	53.43% ± 0.20	–	21.88% ± 0.10	53.31% ± 0.20	–	20.47% ± 0.07
	CPU time (s)	0.298	0.297	–	0.309	0.290	–	0.289
	Min-max normalization	–	–	–	–	–	–	–
	CPU time (s)	–	–	–	–	–	–	–
	Standardization	–	–	–	–	–	–	–
Parkinson	–	<u>19.18% ± 0.10</u>	21.35% ± 0.06	29.75% ± 0.15	55.99% ± 0.36	24.89% ± 0.12	33.57% ± 0.18	19.66% ± 0.03
	CPU time (s)	3.698	3.661	4.402	3.713	3.762	4.259	3.702
	Min-max normalization	13.19% ± 0.03	13.35% ± 0.04	13.95% ± 0.05	13.43% ± 0.05	14.34% ± 0.05	15.23% ± 0.04	13.91% ± 0.04
	CPU time (s)	3.626	3.657	3.636	3.731	3.754	3.656	3.629
	Standardization	14.47% ± 0.04	19.40% ± 0.06	15.95% ± 0.06	16.08% ± 0.06	<u>13.43% ± 0.05</u>	14.11% ± 0.05	16.02% ± 0.05
Heart Disease	–	23.47% ± 0.09	27.79% ± 0.05	37.36% ± 0.08	35.28% ± 0.13	29.77% ± 0.08	40.37% ± 0.09	33.01% ± 0.05
	CPU time (s)	12.102	12.646	13.050	12.296	12.391	12.755	12.333
	Min-max normalization	18.57% ± 0.04	19.82% ± 0.04	22.75% ± 0.05	<u>18.01% ± 0.04</u>	19.75% ± 0.04	22.24% ± 0.05	31.84% ± 0.06
	CPU time (s)	12.115	12.167	12.050	12.124	12.061	12.162	12.749
	Standardization	19.00% ± 0.04	37.27% ± 0.06	23.56% ± 0.04	17.48% ± 0.04	27.48% ± 0.05	24.07% ± 0.04	47.49% ± 0.04
Dermatology	–	5.41% ± 0.06	2.05% ± 0.01	3.03% ± 0.02	6.14% ± 0.07	1.64% ± 0.02	2.90% ± 0.02	7.81% ± 0.08
	CPU time (s)	20.584	20.032	19.969	20.094	20.091	20.033	20.246
	Min-max normalization	3.35% ± 0.03	2.84% ± 0.02	<u>1.85% ± 0.01</u>	3.34% ± 0.03	3.02% ± 0.02	1.95% ± 0.02	30.83% ± 0.01
	CPU time (s)	20.253	20.329	20.173	20.102	20.178	20.132	20.548
	Standardization	<u>3.23% ± 0.03</u>	5.59% ± 0.03	3.29% ± 0.02	3.86% ± 0.03	5.22% ± 0.03	3.35% ± 0.02	30.83% ± 0.01
Climate Model Crashes	–	<u>5.01% ± 0.02</u>	6.04% ± 0.02	8.23% ± 0.02	5.25% ± 0.02	5.87% ± 0.02	7.64% ± 0.02	13.19% ± 0.03
	CPU time (s)	68.069	67.104	65.726	66.070	65.745	66.235	66.383
	Min-max normalization	<u>5.08% ± 0.02</u>	5.52% ± 0.02	7.78% ± 0.02	5.09% ± 0.02	5.87% ± 0.02	7.82% ± 0.03	13.50% ± 0.03
	CPU time (s)	68.296	68.102	69.397	68.228	68.510	69.750	70.330
	Standardization	5.20% ± 0.02	20.15% ± 0.03	11.54% ± 0.02	<u>5.11% ± 0.02</u>	15.73% ± 0.04	11.57% ± 0.03	13.81% ± 0.03
Breast Cancer Diagnostic	–	10.69% ± 0.15	24.85% ± 0.22	–	16.06% ± 0.21	41.46% ± 0.23	–	8.58% ± 0.02
	CPU time (s)	76.706	77.126	–	76.718	78.570	–	80.493
	Min-max normalization	4.12% ± 0.03	3.15% ± 0.02	3.88% ± 0.02	4.39% ± 0.03	3.02% ± 0.02	5.80% ± 0.05	12.87% ± 0.05
	CPU time (s)	76.340	76.476	76.106	76.350	77.786	78.282	77.690
	Standardization	<u>3.65% ± 0.02</u>	17.72% ± 0.03	5.40% ± 0.02	3.88% ± 0.02	6.88% ± 0.02	4.92% ± 0.02	36.62% ± 0.01
Breast Cancer	–	3.21% ± 0.01	7.02% ± 0.02	8.36% ± 0.07	3.39% ± 0.02	6.84% ± 0.02	11.58% ± 0.16	<u>3.20% ± 0.01</u>
	CPU time (s)	133.833	132.231	133.750	134.134	134.697	135.338	133.728
	Min-max normalization	4.06% ± 0.04	3.29% ± 0.01	4.20% ± 0.02	4.12% ± 0.02	4.43% ± 0.03	4.82% ± 0.02	<u>3.20% ± 0.01</u>
	CPU time (s)	135.390	135.382	135.109	137.616	136.871	134.736	136.484
	Standardization	3.17% ± 0.01	6.80% ± 0.03	5.88% ± 0.02	3.19% ± 0.01	6.21% ± 0.02	5.61% ± 0.02	3.88% ± 0.02
Blood Transfusion	–	24.09% ± 0.01	26.57 ± 0.15	–	24.00% ± 0.01	27.35% ± 0.15	–	<u>23.73% ± 0.01</u>
	CPU time (s)	170.744	176.855	–	174.407	176.929	–	174.808
	Min-max normalization	23.82% ± 0.00	23.85% ± 0.01	23.73% ± 0.02	23.84% ± 0.00	23.92% ± 0.01	<u>23.25% ± 0.01</u>	23.53% ± 0.02
	CPU time (s)	176.273	178.011	178.221	177.326	179.052	175.440	176.455
	Standardization	23.85% ± 0.01	23.37% ± 0.01	22.00% ± 0.02	24.01% ± 0.01	20.97% ± 0.02	20.72% ± 0.02	21.09% ± 0.02
Mammographic Mass	–	20.92% ± 0.07	<u>15.85% ± 0.02</u>	17.51% ± 0.05	17.12% ± 0.02	16.20% ± 0.02	28.47% ± 0.15	18.48% ± 0.02
	CPU time (s)	240.550	239.300	241.644	241.607	242.298	242.582	239.141
	Min-max normalization	26.22% ± 0.12	16.60% ± 0.02	16.09% ± 0.02	26.77% ± 0.13	<u>16.04% ± 0.02</u>	16.06% ± 0.02	17.25% ± 0.02
	CPU time (s)	241.645	240.950	239.648	241.134	241.525	239.143	241.536
	Standardization	19.49% ± 0.06	31.14% ± 0.05	18.82% ± 0.03	19.73% ± 0.08	15.71% ± 0.02	18.63% ± 0.02	18.29% ± 0.02
Qsar Biodegradation	–	13.59% ± 0.02	18.36% ± 0.02	18.31% ± 0.05	<u>13.59% ± 0.02</u>	18.31% ± 0.02	18.98% ± 0.02	16.90% ± 0.02
	CPU time (s)	494.464	498.698	500.560	516.170	504.803	602.625	483.529
	Min-max normalization	13.94% ± 0.02	13.03% ± 0.02	14.28% ± 0.02	13.83% ± 0.02	13.09% ± 0.02	14.30% ± 0.02	12.88% ± 0.02
	CPU time (s)	490.659	492.560	493.424	494.058	492.735	491.389	484.908
	Standardization	13.58% ± 0.02	19.10% ± 0.02	18.35% ± 0.02	<u>13.31% ± 0.02</u>	17.87% ± 0.02	18.01% ± 0.03	20.69% ± 0.03
CPU time (s)	491.943	493.024	489.466	491.152	512.859	524.465	519.287	

Table B.7: Detailed results of average out-of-sample testing errors and standard deviations over 96 runs of the deterministic model. Holdout: 75% training set-25% testing set.

Dataset	Data transformation	Kernel						
		Hom. linear	Hom. quadratic	Hom. cubic	Inhom. linear	Inhom. quadratic	Inhom. cubic	Gaussian RBF
Arrhythmia	–	23.90% ± 0.06	54.23% ± 0.02	–	24.08% ± 0.05	51.72% ± 0.21	–	23.59% ± 0.04
	CPU time (s)	0.194	0.180	–	0.191	0.216	–	0.181
	Min-max normalization	–	–	–	–	–	–	–
	CPU time (s)	–	–	–	–	–	–	–
	Standardization	–	–	–	–	–	–	–
Parkinson	–	19.58% ± 0.11	25.10% ± 0.06	40.05% ± 0.22	46.88% ± 0.27	23.70% ± 0.07	32.07% ± 0.17	19.97% ± 0.05
	CPU time (s)	1.283	1.230	1.290	1.211	1.330	1.382	1.264
	Min-max normalization	15.54% ± 0.06	15.10% ± 0.04	16.02% ± 0.04	15.43% ± 0.04	16.26% ± 0.04	16.13% ± 0.04	18.38% ± 0.04
	CPU time (s)	1.195	1.203	1.206	1.214	1.202	1.207	1.184
	Standardization	<u>15.79% ± 0.04</u>	22.71% ± 0.06	17.74% ± 0.05	17.62% ± 0.04	17.98% ± 0.04	17.71% ± 0.05	19.33% ± 0.05
Heart Disease	–	23.00% ± 0.08	28.55% ± 0.04	37.81% ± 0.07	31.07% ± 0.13	30.36% ± 0.07	42.13% ± 0.09	34.45% ± 0.04
	CPU time (s)	4.132	4.199	4.732	4.193	4.223	4.821	4.045
	Min-max normalization	20.00% ± 0.03	21.40% ± 0.03	22.87% ± 0.04	20.11% ± 0.06	20.82% ± 0.03	22.64% ± 0.03	32.07% ± 0.06
	CPU time (s)	4.078	4.076	4.097	4.063	4.098	4.168	4.057
	Standardization	19.05% ± 0.04	37.16% ± 0.04	23.97% ± 0.03	18.92% ± 0.03	26.82% ± 0.04	23.99% ± 0.04	46.01% ± 0.04
Dermatology	–	8.90% ± 0.08	2.01% ± 0.01	3.17% ± 0.02	12.08% ± 0.11	1.96% ± 0.01	3.34% ± 0.02	8.82% ± 0.08
	CPU time (s)	5.999	6.015	6.115	6.089	6.075	6.072	6.115
	Min-max normalization	4.35% ± 0.05	3.45% ± 0.02	2.55% ± 0.02	4.82% ± 0.06	3.93% ± 0.02	<u>2.42% ± 0.01</u>	30.97% ± 0.00
	CPU time (s)	6.019	6.159	6.049	6.077	6.090	6.021	6.137
	Standardization	4.16% ± 0.03	7.16% ± 0.02	4.19% ± 0.02	4.78% ± 0.03	5.74% ± 0.02	<u>4.14% ± 0.02</u>	30.97% ± 0.00
Climate Model Crashes	–	5.56% ± 0.01	7.01% ± 0.02	8.16% ± 0.02	5.35% ± 0.01	7.44% ± 0.02	8.23% ± 0.02	13.42% ± 0.02
	CPU time (s)	20.032	20.018	20.056	20.035	20.051	20.145	19.856
	Min-max normalization	5.57% ± 0.01	7.21% ± 0.02	8.24% ± 0.02	<u>5.42% ± 0.01</u>	7.17% ± 0.02	8.29% ± 0.02	13.57% ± 0.02
	CPU time (s)	20.742	21.174	20.553	20.941	20.628	20.147	20.740
	Standardization	<u>5.82% ± 0.01</u>	20.01% ± 0.03	11.77% ± 0.02	6.40% ± 0.02	15.21% ± 0.03	11.55% ± 0.03	13.14% ± 0.02
Breast Cancer Diagnostic	–	13.53% ± 0.18	27.06% ± 0.24	–	16.94% ± 0.23	34.81% ± 0.23	–	<u>9.26% ± 0.02</u>
	CPU time (s)	24.553	24.289	–	24.410	24.671	–	24.525
	Min-max normalization	6.21% ± 0.06	3.87% ± 0.03	4.43% ± 0.01	5.99% ± 0.05	3.69% ± 0.02	5.19% ± 0.03	20.68% ± 0.08
	CPU time (s)	24.449	24.405	24.600	24.671	24.237	24.634	23.636
	Standardization	<u>4.17% ± 0.02</u>	19.01% ± 0.02	5.67% ± 0.02	4.45% ± 0.03	7.43% ± 0.02	5.22% ± 0.01	37.21% ± 0.00
Breast Cancer	–	4.54% ± 0.04	6.47% ± 0.02	12.57% ± 0.11	<u>3.61% ± 0.02</u>	6.72% ± 0.01	26.05% ± 0.25	3.84% ± 0.01
	CPU time (s)	39.279	39.238	40.161	38.794	40.341	39.618	39.730
	Min-max normalization	5.71% ± 0.06	3.31% ± 0.01	4.52% ± 0.01	10.05% ± 0.11	4.37% ± 0.02	4.99% ± 0.01	3.62% ± 0.01
	CPU time (s)	38.718	40.067	39.394	39.775	39.780	39.395	42.094
	Standardization	<u>3.37% ± 0.01</u>	7.69% ± 0.02	6.13% ± 0.01	3.75% ± 0.01	6.43% ± 0.01	5.97% ± 0.01	5.08% ± 0.02
Blood Transfusion	–	23.81% ± 0.01	<u>22.99% ± 0.01</u>	–	23.68% ± 0.00	31.60% ± 0.19	–	25.40% ± 0.09
	CPU time (s)	49.452	50.652	–	51.609	54.469	–	51.579
	Min-max normalization	23.85% ± 0.00	23.84% ± 0.01	23.69% ± 0.01	23.81% ± 0.00	23.77% ± 0.01	23.59% ± 0.01	23.38% ± 0.01
	CPU time (s)	51.422	51.582	52.451	52.365	51.648	52.098	51.996
	Standardization	23.77% ± 0.01	23.77% ± 0.01	22.52% ± 0.01	23.69% ± 0.00	21.98% ± 0.01	21.86% ± 0.03	22.07% ± 0.01
Mammographic Mass	–	24.02% ± 0.10	<u>17.28% ± 0.05</u>	35.66% ± 0.16	25.55% ± 0.11	40.95% ± 0.14	46.42% ± 0.09	19.84 ± 0.02
	CPU time (s)	70.958	70.916	71.854	71.198	72.179	72.495	70.880
	Min-max normalization	21.74% ± 0.09	17.72% ± 0.02	16.49% ± 0.02	23.36% ± 0.11	19.71% ± 0.08	18.62% ± 0.08	17.94% ± 0.01
	CPU time (s)	71.468	71.291	71.426	71.415	71.274	73.143	71.589
	Standardization	20.08% ± 0.06	32.87% ± 0.07	19.86% ± 0.02	20.25% ± 0.06	<u>16.56% ± 0.01</u>	19.54% ± 0.02	18.84% ± 0.02
Qsar Biodegradation	–	<u>14.14% ± 0.01</u>	19.09% ± 0.02	20.03% ± 0.02	14.19% ± 0.01	18.70% ± 0.02	19.57% ± 0.02	17.35% ± 0.01
	CPU time (s)	148.271	149.795	151.266	149.400	151.116	194.702	147.980
	Min-max normalization	14.99% ± 0.02	13.67% ± 0.01	14.96% ± 0.02	13.76% ± 0.01	14.62% ± 0.01	15.00% ± 0.02	13.83% ± 0.01
	CPU time (s)	149.522	147.227	160.539	149.207	149.145	149.296	147.803
	Standardization	<u>14.33% ± 0.01</u>	19.85 ± 0.02	19.50 ± 0.02	<u>14.33% ± 0.01</u>	19.06% ± 0.02	18.56% ± 0.02	20.56% ± 0.04
CPU time (s)	148.379	147.027	148.483	148.837	149.612	149.612	146.024	

Table B.8: Detailed results of average out-of-sample testing errors and standard deviations over 96 runs of the deterministic model. Holdout: 50% training set-50% testing set.

Dataset	Data transformation	Kernel						
		Hom. linear	Hom. quadratic	Hom. cubic	Inhom. linear	Inhom. quadratic	Inhom. cubic	Gaussian RBF
Arrhythmia	–	28.66% ± 0.07	53.45% ± 0.20	–	27.31% ± 0.07	53.84% ± 0.20	–	28.29% ± 0.02
	CPU time (s)	0.142	0.165	–	0.144	0.148	–	0.153
	Min-max normalization	–	–	–	–	–	–	–
	CPU time (s)	–	–	–	–	–	–	–
	Standardization	–	–	–	–	–	–	–
Parkinson	–	26.58% ± 0.17	25.55% ± 0.05	45.19% ± 0.24	37.54% ± 0.25	25.85% ± 0.08	45.44% ± 0.25	<u>21.48% ± 0.03</u>
	CPU time (s)	0.293	0.303	0.530	0.301	0.285	0.596	0.295
	Min-max normalization	18.91% ± 0.05	18.49% ± 0.04	20.92% ± 0.05	19.98% ± 0.06	19.66% ± 0.07	21.08% ± 0.06	21.88% ± 0.04
	CPU time (s)	0.311	0.286	0.281	0.291	0.294	0.301	0.291
	Standardization	20.03% ± 0.04	30.18% ± 0.05	23.10% ± 0.06	<u>19.73% ± 0.04</u>	23.47% ± 0.06	22.85% ± 0.05	23.78% ± 0.05
Heart Disease	–	<u>25.58% ± 0.08</u>	28.73% ± 0.04	42.38% ± 0.08	28.03% ± 0.10	29.50% ± 0.06	46.02% ± 0.08	36.61% ± 0.04
	CPU time (s)	0.656	0.648	1.496	0.703	0.682	1.863	0.613
	Min-max normalization	22.00% ± 0.05	23.18% ± 0.03	22.76% ± 0.03	21.85% ± 0.05	23.33% ± 0.04	23.07% ± 0.03	38.86% ± 0.07
	CPU time (s)	0.638	0.640	0.663	0.625	0.628	0.640	0.634
	Standardization	<u>22.48% ± 0.04</u>	39.13% ± 0.04	25.48% ± 0.04	22.94% ± 0.06	28.38% ± 0.03	25.67% ± 0.04	45.74% ± 0.03
Dermatology	–	13.17% ± 0.11	<u>3.13% ± 0.02</u>	4.19% ± 0.03	13.88% ± 0.11	3.14% ± 0.02	4.18% ± 0.04	10.01% ± 0.04
	CPU time (s)	0.971	0.981	0.963	0.956	0.951	0.965	0.974
	Min-max normalization	10.32% ± 0.11	5.81% ± 0.05	3.65% ± 0.02	9.03% ± 0.10	5.66% ± 0.05	3.01% ± 0.02	30.97% ± 0.00
	CPU time (s)	1.006	1.100	0.958	0.960	0.960	0.977	0.957
	Standardization	<u>6.74% ± 0.04</u>	10.54% ± 0.03	7.35% ± 0.03	7.97% ± 0.05	9.52% ± 0.03	7.05% ± 0.03	30.97% ± 0.00
Climate Model Crashes	–	7.28% ± 0.01	10.51% ± 0.02	10.47% ± 0.02	7.15% ± 0.01	10.59% ± 0.03	11.18% ± 0.03	14.34% ± 0.02
	CPU time (s)	2.804	2.715	2.686	2.671	2.653	2.662	2.811
	Min-max normalization	<u>7.20% ± 0.01</u>	10.54% ± 0.02	10.80% ± 0.03	7.27% ± 0.01	10.77% ± 0.03	10.66% ± 0.03	14.14% ± 0.02
	CPU time (s)	2.847	2.827	2.840	2.848	2.865	2.856	2.839
	Standardization	10.04% ± 0.03	19.74% ± 0.05	12.58% ± 0.04	<u>9.99% ± 0.03</u>	14.36% ± 0.04	12.53% ± 0.03	13.51% ± 0.02
Breast Cancer Diagnostic	–	17.25% ± 0.19	39.75% ± 0.24	–	20.31% ± 0.23	28.03% ± 0.23	–	<u>11.21% ± 0.04</u>
	CPU time (s)	3.498	3.515	–	3.256	3.419	–	3.376
	Min-max normalization	8.62% ± 0.07	6.29% ± 0.05	5.98% ± 0.02	8.89% ± 0.08	<u>5.87% ± 0.04</u>	6.43% ± 0.03	33.15% ± 0.06
	CPU time (s)	3.439	3.249	3.285	3.289	3.250	3.255	3.395
	Standardization	5.11% ± 0.02	22.85% ± 0.03	6.37% ± 0.02	5.02% ± 0.02	10.49% ± 0.02	6.17% ± 0.02	37.32% ± 0.00
Breast Cancer	–	7.05% ± 0.06	6.58% ± 0.02	21.30% ± 0.14	6.56% ± 0.06	6.73% ± 0.02	21.95% ± 0.20	<u>5.00% ± 0.02</u>
	CPU time (s)	5.392	5.318	5.406	5.440	5.490	5.506	5.511
	Min-max normalization	8.62% ± 0.09	4.47% ± 0.02	5.92% ± 0.02	11.70% ± 0.11	5.01% ± 0.04	5.83% ± 0.02	5.00% ± 0.02
	CPU time (s)	5.507	5.536	5.574	5.420	5.463	5.522	5.505
	Standardization	5.12% ± 0.05	9.45% ± 0.02	6.36% ± 0.02	<u>4.64% ± 0.03</u>	7.33% ± 0.02	6.18% ± 0.02	6.01% ± 0.02
Blood Transfusion	–	23.69% ± 0.00	<u>23.55% ± 0.01</u>	–	23.69% ± 0.01	42.69% ± 0.25	–	23.96% ± 0.01
	CPU time (s)	7.214	7.618	–	7.342	7.622	–	6.838
	Min-max normalization	23.85% ± 0.01	23.75% ± 0.01	23.69% ± 0.01	23.77% ± 0.00	23.68% ± 0.00	23.68% ± 0.01	<u>23.53% ± 0.01</u>
	CPU time (s)	7.319	7.430	7.141	7.398	7.122	7.144	6.665
	Standardization	23.75% ± 0.01	23.63% ± 0.00	23.32% ± 0.01	23.72% ± 0.00	23.37% ± 0.05	26.03% ± 0.09	23.35% ± 0.01
Mammographic Mass	–	28.35% ± 0.13	<u>18.83% ± 0.05</u>	37.40% ± 0.14	30.20% ± 0.14	36.33% ± 0.15	39.55% ± 0.15	22.21% ± 0.03
	CPU time (s)	9.024	9.013	9.166	9.206	9.152	9.166	8.964
	Min-max normalization	22.21% ± 0.09	19.02% ± 0.04	17.68% ± 0.02	24.31% ± 0.11	19.56% ± 0.05	20.38% ± 0.08	19.39% ± 0.02
	CPU time (s)	9.068	9.086	9.116	9.019	9.009	9.021	8.953
	Standardization	19.48% ± 0.04	32.89% ± 0.09	21.98% ± 0.04	21.02% ± 0.06	<u>19.21% ± 0.04</u>	24.04% ± 0.07	20.13% ± 0.02
Qsar Biodegradation	–	16.34% ± 0.02	20.76% ± 0.02	21.33% ± 0.02	<u>16.12% ± 0.02</u>	20.74% ± 0.02	21.33% ± 0.02	20.05% ± 0.02
	CPU time (s)	18.825	18.691	23.396	18.423	18.642	22.609	18.546
	Min-max normalization	16.60% ± 0.01	15.29% ± 0.01	16.70% ± 0.02	16.60% ± 0.01	15.45% ± 0.01	16.85% ± 0.02	15.93% ± 0.01
	CPU time (s)	18.698	19.085	19.739	19.355	19.758	19.698	18.355
	Standardization	<u>16.01% ± 0.01</u>	22.33% ± 0.02	21.78% ± 0.02	16.10% ± 0.02	20.47% ± 0.02	20.87% ± 0.02	20.79% ± 0.04
CPU time (s)	18.549	19.021	19.535	19.518	19.050	19.623	18.509	

Table B.9: Detailed results of average out-of-sample testing errors and standard deviations over 96 runs of the deterministic model. Holdout: 25% training set-75% testing set.

Dataset	Data transformation	Kernel						
		Hom. linear	Hom. quadratic	Hom. cubic	Inhom. linear	Inhom. quadratic	Inhom. cubic	Gaussian RBF
Iris	–	6.42% ± 0.04	3.89% ± 0.03	5.83% ± 0.03	6.53% ± 0.04	4.28% ± 0.04	6.39% ± 0.04	3.10% ± 0.03
	CPU time (s)	5.470	5.547	5.485	5.461	5.454	5.497	5.391
	Min-max normalization	10.92% ± 0.08	8.31% ± 0.07	6.02% ± 0.04	11.20% ± 0.08	5.74% ± 0.03	5.01% ± 0.03	4.28% ± 0.03
	CPU time (s)	5.131	5.130	5.031	5.104	5.123	5.088	5.122
	Standardization	8.70% ± 0.05	15.20% ± 0.06	8.61% ± 0.5	8.70% ± 0.05	6.11% ± 0.04	7.74% ± 0.04	5.32% ± 0.03
	CPU time (s)	5.476	5.374	5.307	5.087	5.172	5.105	5.121
Wine	–	4.62% ± 0.02	3.67% ± 0.02	9.26% ± 0.06	4.62% ± 0.03	3.93% ± 0.03	10.23% ± 0.07	33.97% ± 0.03
	CPU time (s)	7.955	8.088	10.849	8.050	7.983	10.758	8.006
	Min-max normalization	3.55% ± 0.03	3.01% ± 0.02	3.24% ± 0.03	3.84% ± 0.03	2.79% ± 0.02	3.27% ± 0.03	9.80% ± 0.05
	CPU time (s)	7.977	8.074	8.034	8.035	8.064	8.049	8.149
	Standardization	3.48% ± 0.02	11.86% ± 0.05	4.88% ± 0.03	2.77% ± 0.02	5.45% ± 0.03	4.40% ± 0.03	4.24% ± 0.07
	CPU time (s)	7.957	7.907	7.919	7.916	7.922	8.088	7.983

Table B.10: Detailed results of average out-of-sample testing errors and standard deviations over 96 runs of the deterministic multiclass model. Holdout: 75% training set-25% testing set.

Dataset	Data transformation	Kernel						
		Hom. linear	Hom. quadratic	Hom. cubic	Inhom. linear	Inhom. quadratic	Inhom. cubic	Gaussian RBF
Iris	–	6.79% ± 0.05	5.08% ± 0.02	6.33% ± 0.03	6.63% ± 0.05	4.63% ± 0.03	5.97% ± 0.03	4.58% ± 0.03
	CPU time (s)	1.938	1.942	2.042	1.936	2.123	1.982	1.958
	Min-max normalization	22.04% ± 0.11	23.43% ± 0.10	9.21% ± 0.06	20.13% ± 0.11	12.74% ± 0.09	5.44% ± 0.02	4.47% ± 0.02
	CPU time (s)	1.808	1.798	1.784	1.794	1.819	1.793	1.828
	Standardization	10.89% ± 0.06	19.56% ± 0.04	10.06% ± 0.05	9.65% ± 0.05	6.92% ± 0.02	7.60% ± 0.03	5.75% ± 0.03
	CPU time (s)	1.913	1.906	1.841	1.832	1.797	1.979	1.951
Wine	–	4.58% ± 0.02	5.13% ± 0.03	33.58% ± 0.08	4.73% ± 0.02	5.37% ± 0.03	35.33% ± 0.09	34.89% ± 0.04
	CPU time (s)	2.760	2.760	3.569	2.731	2.750	3.753	2.795
	Min-max normalization	4.33% ± 0.02	3.78% ± 0.02	3.98% ± 0.02	4.59% ± 0.02	3.98% ± 0.02	3.82% ± 0.02	10.56% ± 0.08
	CPU time (s)	2.795	2.756	2.767	2.732	2.730	2.854	2.795
	Standardization	3.55% ± 0.02	14.28% ± 0.03	6.48% ± 0.03	3.69% ± 0.02	6.04% ± 0.02	6.00% ± 0.03	4.14% ± 0.06
	CPU time (s)	2.743	2.728	2.739	2.736	2.735	2.742	2.777

Table B.11: Detailed results of average out-of-sample testing errors and standard deviations over 96 runs of the deterministic multiclass model. Holdout: 50% training set-50% testing set.

Dataset	Data transformation	Kernel						
		Hom. linear	Hom. quadratic	Hom. cubic	Inhom. linear	Inhom. quadratic	Inhom. cubic	Gaussian RBF
Iris	–	11.90% ± 0.09	5.30% ± 0.03	5.51% ± 0.03	11.21% ± 0.08	5.05% ± 0.03	5.57% ± 0.03	8.28% ± 0.03
	CPU time (s)	0.645	0.635	0.603	0.591	0.728	0.645	0.606
	Min-max normalization	28.25% ± 0.08	30.50% ± 0.06	27.10% ± 0.09	28.51% ± 0.08	24.73% ± 0.09	10.75% ± 0.07	7.33% ± 0.04
	CPU time (s)	0.589	0.590	0.567	0.685	0.559	0.560	0.570
	Standardization	13.45% ± 0.08	25.29% ± 0.05	15.34% ± 0.06	13.24% ± 0.07	7.70% ± 0.03	8.66% ± 0.03	8.54% ± 0.04
	CPU time (s)	0.590	0.611	0.628	0.590	0.698	0.574	0.581
Wine	–	7.69% ± 0.03	7.94% ± 0.04	47.10% ± 0.08	8.24% ± 0.03	7.74% ± 0.04	48.43% ± 0.09	33.02% ± 0.02
	CPU time (s)	0.730	0.747	0.776	0.725	0.854	0.832	0.733
	Min-max normalization	5.74% ± 0.03	5.72% ± 0.03	6.64% ± 0.03	5.98% ± 0.03	6.02% ± 0.02	6.67% ± 0.03	7.83% ± 0.08
	CPU time (s)	0.767	0.743	0.755	0.704	0.735	0.850	0.704
	Standardization	5.14% ± 0.02	18.80% ± 0.04	10.60% ± 0.04	4.89% ± 0.02	8.47% ± 0.03	9.30% ± 0.04	4.43% ± 0.04
	CPU time (s)	0.731	0.735	0.715	0.700	0.708	0.712	0.707

Table B.12: Detailed results of average out-of-sample testing errors and standard deviations over 96 runs of the deterministic multiclass model. Holdout: 25% training set-75% testing set.

Dataset	Data transformation	Kernel	ρ	Robust		
				$p = 1$	$p = 2$	$p = \infty$
Arrhythmia	-	Gaussian RBF	10^{-7}	$19.18\% \pm 0.07$	$19.42\% \pm 0.07$	$19.67\% \pm 0.07$
			10^{-6}	$19.30\% \pm 0.06$	$19.61\% \pm 0.07$	$20.40\% \pm 0.08$
			10^{-5}	$20.47\% \pm 0.07$	$19.91\% \pm 0.07$	$19.73\% \pm 0.06$
			10^{-4}	$20.10\% \pm 0.07$	$19.55\% \pm 0.07$	$19.61\% \pm 0.07$
			10^{-3}	$19.12\% \pm 0.08$	$19.30\% \pm 0.07$	$23.28\% \pm 0.06$
			10^{-2}	$19.30\% \pm 0.07$	$20.83\% \pm 0.08$	$29.41\% \pm 0.00$
			10^{-1}	$29.41\% \pm 0.00$	$29.41\% \pm 0.00$	$29.41\% \pm 0.00$
			CPU time (s)	0.290	0.288	0.295
Parkinson	Min-max normalization	Hom. linear	10^{-7}	<u>$12.98\% \pm 0.03$</u>	$12.87\% \pm 0.03$	$13.02\% \pm 0.04$
			10^{-6}	$13.50\% \pm 0.04$	$13.02\% \pm 0.04$	$12.80\% \pm 0.04$
			10^{-5}	$13.04\% \pm 0.04$	$13.28\% \pm 0.04$	<u>$12.61\% \pm 0.04$</u>
			10^{-4}	$13.93\% \pm 0.03$	$12.37\% \pm 0.03$	$12.72\% \pm 0.03$
			10^{-3}	$13.54\% \pm 0.03$	<u>$13.32\% \pm 0.04$</u>	$13.48\% \pm 0.04$
			10^{-2}	$12.98\% \pm 0.03$	$13.17\% \pm 0.04$	$15.15\% \pm 0.04$
			10^{-1}	$15.28\% \pm 0.03$	$15.58\% \pm 0.03$	$25.00\% \pm 0.00$
			CPU time (s)	3.421	3.454	3.418
Heart disease	Standardization	Inhom. linear	10^{-7}	<u>$16.84\% \pm 0.04$</u>	$17.53\% \pm 0.04$	$16.84\% \pm 0.04$
			10^{-6}	$17.53\% \pm 0.04$	$17.72\% \pm 0.04$	$17.53\% \pm 0.04$
			10^{-5}	$17.37\% \pm 0.04$	$18.26\% \pm 0.03$	$17.38\% \pm 0.04$
			10^{-4}	$17.75\% \pm 0.04$	$18.27\% \pm 0.04$	$17.64\% \pm 0.04$
			10^{-3}	$17.13\% \pm 0.04$	$18.43\% \pm 0.04$	$17.12\% \pm 0.04$
			10^{-2}	$17.10\% \pm 0.04$	$17.92\% \pm 0.04$	$16.36\% \pm 0.04$
			10^{-1}	$16.98\% \pm 0.04$	<u>$17.53\% \pm 0.03$</u>	$16.37\% \pm 0.04$
			CPU time (s)	11.602	11.477	11.417
Dermatology	-	Inhom. quadratic	10^{-7}	<u>$1.65\% \pm 0.01$</u>	$1.71\% \pm 0.01$	$1.72\% \pm 0.01$
			10^{-6}	$1.78\% \pm 0.01$	$1.80\% \pm 0.02$	$1.79\% \pm 0.01$
			10^{-5}	$1.73\% \pm 0.02$	<u>$1.57\% \pm 0.01$</u>	$1.76\% \pm 0.01$
			10^{-4}	$11.06\% \pm 0.04$	$0.39\% \pm 0.04$	$1.28\% \pm 0.01$
			10^{-3}	$30.93\% \pm 0.01$	$30.93\% \pm 0.01$	$0.55\% \pm 0.01$
			10^{-2}	$30.91\% \pm 0.01$	$30.86\% \pm 0.01$	$30.89\% \pm 0.01$
			10^{-1}	$38.06\% \pm 0.21$	$32.33\% \pm 0.10$	$30.92\% \pm 0.01$
			CPU time (s)	20.055	20.420	20.147
Climate Model Crashes	-	Hom. linear	10^{-7}	$4.74\% \pm 0.02$	$4.51\% \pm 0.01$	$4.60\% \pm 0.02$
			10^{-6}	$4.70\% \pm 0.02$	$4.88\% \pm 0.01$	$4.93\% \pm 0.02$
			10^{-5}	$4.52\% \pm 0.02$	$4.56\% \pm 0.01$	$4.71\% \pm 0.02$
			10^{-4}	$4.86\% \pm 0.02$	$4.78\% \pm 0.02$	$4.85\% \pm 0.01$
			10^{-3}	<u>$4.47\% \pm 0.02$</u>	$4.71\% \pm 0.01$	$4.34\% \pm 0.01$
			10^{-2}	$4.67\% \pm 0.01$	<u>$4.50\% \pm 0.01$</u>	$4.81\% \pm 0.02$
			10^{-1}	$8.46\% \pm 0.00$	$8.52\% \pm 0.00$	$8.47\% \pm 0.00$
			CPU time (s)	66.762	67.169	67.381

Table B.13: Average out-of-sample testing errors and standard deviations over 96 runs of the robust model. Holdout: 75% training set-25% testing set.

Dataset	Data transformation	Kernel	ρ	Robust		
				$p = 1$	$p = 2$	$p = \infty$
Breast Cancer Diagnostic	Min-max normalization	Inhom. quadratic	10^{-7}	$2.80\% \pm 0.01$	<u>$2.65\% \pm 0.01$</u>	$2.80\% \pm 0.01$
			10^{-6}	$2.96\% \pm 0.02$	$2.70\% \pm 0.01$	$2.96\% \pm 0.02$
			10^{-5}	<u>$2.63\% \pm 0.01$</u>	$2.99\% \pm 0.01$	$2.66\% \pm 0.01$
			10^{-4}	$2.88\% \pm 0.01$	$2.88\% \pm 0.01$	<u>$2.39\% \pm 0.01$</u>
			10^{-3}	$2.91\% \pm 0.01$	$3.19\% \pm 0.01$	$9.76\% \pm 0.03$
			10^{-2}	$37.32\% \pm 0.00$	$37.32\% \pm 0.00$	$37.32\% \pm 0.00$
			10^{-1}	$37.32\% \pm 0.00$	$37.32\% \pm 0.00$	$37.32\% \pm 0.00$
			CPU time (s)	77.968	78.267	77.543
			Breast Cancer	Standardization	Hom. linear	10^{-7}
10^{-6}	$3.16\% \pm 0.01$	$3.26\% \pm 0.01$				$3.17\% \pm 0.01$
10^{-5}	<u>$2.97\% \pm 0.01$</u>	$3.32\% \pm 0.01$				$3.14\% \pm 0.01$
10^{-4}	$3.23\% \pm 0.01$	$3.50\% \pm 0.01$				$3.20\% \pm 0.01$
10^{-3}	$3.11\% \pm 0.01$	<u>$3.07\% \pm 0.01$</u>				$3.21\% \pm 0.01$
10^{-2}	$3.33\% \pm 0.01$	$3.19\% \pm 0.01$				$3.08\% \pm 0.01$
10^{-1}	$3.07\% \pm 0.01$	$3.32\% \pm 0.01$				<u>$3.06\% \pm 0.01$</u>
CPU time (s)	135.651	137.039				136.286
Blood Transfusion	Standardization	Inhom. cubic				10^{-7}
			10^{-6}	$20.72\% \pm 0.02$	$20.80\% \pm 0.02$	$20.77\% \pm 0.02$
			10^{-5}	$21.26\% \pm 0.02$	$20.97\% \pm 0.02$	$22.49\% \pm 0.02$
			10^{-4}	$23.88\% \pm 0.00$	$23.85\% \pm 0.00$	$23.79\% \pm 0.00$
			10^{-3}	$23.80\% \pm 0.00$	$24.57\% \pm 0.08$	$26.18\% \pm 0.13$
			10^{-2}	$26.19\% \pm 0.13$	$30.94\% \pm 0.22$	$38.88\% \pm 0.31$
			10^{-1}	$61.12\% \pm 0.38$	$57.13\% \pm 0.38$	$56.37\% \pm 0.38$
			CPU time (s)	178.751	179.682	180.083
			Mammographic Mass	Standardization	Inhom. quadratic	10^{-7}
10^{-6}	$15.57\% \pm 0.02$	$15.46\% \pm 0.03$				$15.74\% \pm 0.03$
10^{-5}	<u>$15.49\% \pm 0.02$</u>	$16.16\% \pm 0.03$				$15.66\% \pm 0.02$
10^{-4}	$15.91\% \pm 0.02$	$16.16\% \pm 0.03$				$18.81\% \pm 0.02$
10^{-3}	$48.54\% \pm 0.00$	$48.56\% \pm 0.00$				$48.56\% \pm 0.00$
10^{-2}	$48.57\% \pm 0.00$	$48.53\% \pm 0.00$				$48.53\% \pm 0.00$
10^{-1}	$48.56\% \pm 0.00$	$48.54\% \pm 0.00$				$48.54\% \pm 0.00$
CPU time (s)	241.810	242.614				241.929
Qsar Biodegradation	Min-max normalization	Gaussian RBF				10^{-7}
			10^{-6}	$12.67\% \pm 0.02$	$12.86\% \pm 0.02$	<u>$12.86\% \pm 0.02$</u>
			10^{-5}	$12.60\% \pm 0.02$	$12.94\% \pm 0.02$	$13.05\% \pm 0.02$
			10^{-4}	$12.73\% \pm 0.01$	$13.04\% \pm 0.01$	$13.05\% \pm 0.02$
			10^{-3}	$12.83\% \pm 0.03$	<u>$12.72\% \pm 0.02$</u>	$14.02\% \pm 0.02$
			10^{-2}	$14.68\% \pm 0.02$	$14.89\% \pm 0.02$	$25.90\% \pm 0.04$
			10^{-1}	$33.84\% \pm 0.00$	$33.84\% \pm 0.00$	$33.84\% \pm 0.00$
			CPU time (s)	498.235	495.073	491.748

Table B.14: Average out-of-sample testing errors and standard deviations over 96 runs of the robust model. Holdout: 75% training set-25% testing set (continued).

Dataset	Data transformation	Kernel	ρ	Robust		
				$p = 1$	$p = 2$	$p = \infty$
Arrhythmia	-	Gaussian RBF	10^{-7}	24.66% \pm 0.04	23.99% \pm 0.05	23.44% \pm 0.04
			10^{-6}	24.11% \pm 0.05	24.63% \pm 0.04	23.77% \pm 0.05
			10^{-5}	23.81% \pm 0.05	24.08% \pm 0.04	24.11% \pm 0.05
			10^{-4}	<u>23.77% \pm 0.05</u>	<u>23.74% \pm 0.05</u>	24.33% \pm 0.05
			10^{-3}	24.51% \pm 0.04	24.60% \pm 0.05	26.10% \pm 0.04
			10^{-2}	24.36% \pm 0.04	23.77% \pm 0.05	29.41% \pm 0.00
			10^{-1}	29.41% \pm 0.00	29.41% \pm 0.00	29.41% \pm 0.00
			CPU time (s)	0.191	0.195	0.196
Parkinson	Min-max normalization	Hom. quadratic	10^{-7}	13.92% \pm 0.03	14.89% \pm 0.04	14.51% \pm 0.03
			10^{-6}	14.85% \pm 0.03	14.45% \pm 0.03	14.25% \pm 0.03
			10^{-5}	14.52% \pm 0.03	14.45% \pm 0.03	14.45% \pm 0.03
			10^{-4}	14.28% \pm 0.04	14.28% \pm 0.03	14.33% \pm 0.03
			10^{-3}	14.84% \pm 0.03	14.41% \pm 0.03	<u>13.85% \pm 0.03</u>
			10^{-2}	13.84% \pm 0.03	13.86% \pm 0.03	15.01% \pm 0.03
			10^{-1}	15.38% \pm 0.02	15.70% \pm 0.02	24.74% \pm 0.00
			CPU time (s)	1.195	1.217	1.224
Heart disease	Standardization	Inhom. linear	10^{-7}	18.38% \pm 0.03	18.21% \pm 0.02	18.21% \pm 0.02
			10^{-6}	18.18% \pm 0.03	18.53% \pm 0.03	18.53% \pm 0.03
			10^{-5}	17.98% \pm 0.03	18.17% \pm 0.03	18.17% \pm 0.03
			10^{-4}	18.29% \pm 0.03	18.82% \pm 0.03	18.78% \pm 0.03
			10^{-3}	18.88% \pm 0.03	18.19% \pm 0.03	18.19% \pm 0.03
			10^{-2}	18.92% \pm 0.03	18.22% \pm 0.03	18.05% \pm 0.03
			10^{-1}	<u>17.34% \pm 0.02</u>	<u>17.65% \pm 0.02</u>	17.29% \pm 0.02
			CPU time (s)	3.686	3.795	3.766
Dermatology	-	Inhom. quadratic	10^{-7}	1.97% \pm 0.01	2.19% \pm 0.01	1.97% \pm 0.01
			10^{-6}	1.93% \pm 0.01	1.96% \pm 0.01	1.93% \pm 0.01
			10^{-5}	1.98% \pm 0.01	2.38% \pm 0.01	1.94% \pm 0.01
			10^{-4}	2.04% \pm 0.01	2.12% \pm 0.01	1.71% \pm 0.01
			10^{-3}	1.55% \pm 0.01	1.40% \pm 0.01	<u>0.73% \pm 0.01</u>
			10^{-2}	<u>0.62% \pm 0.01</u>	0.51% \pm 0.01	31.00% \pm 0.00
			10^{-1}	31.02% \pm 0.00	30.98% \pm 0.00	31.02% \pm 0.00
			CPU time (s)	6.156	6.178	6.200
Climate Model Crashes	-	Inhom. linear	10^{-7}	5.27% \pm 0.01	5.23% \pm 0.01	5.23% \pm 0.01
			10^{-6}	<u>5.23% \pm 0.01</u>	5.27% \pm 0.01	5.27% \pm 0.01
			10^{-5}	5.35% \pm 0.01	5.35% \pm 0.01	5.34% \pm 0.01
			10^{-4}	5.46% \pm 0.01	5.28% \pm 0.01	<u>5.23% \pm 0.01</u>
			10^{-3}	5.43% \pm 0.01	5.21% \pm 0.01	5.41% \pm 0.01
			10^{-2}	5.46% \pm 0.01	5.44% \pm 0.01	6.30% \pm 0.01
			10^{-1}	8.51% \pm 0.00	8.52% \pm 0.00	8.52% \pm 0.00
			CPU time (s)	19.874	20.420	19.868

Table B.15: Average out-of-sample testing errors and standard deviations over 96 runs of the robust model. Holdout: 50% training set-50% testing set.

Dataset	Data transformation	Kernel	ρ	Robust		
				$p = 1$	$p = 2$	$p = \infty$
Breast Cancer Diagnostic	Min-max normalization	Inhom. quadratic	10^{-7}	3.06% \pm 0.01	3.19% \pm 0.01	3.06% \pm 0.01
			10^{-6}	3.19% \pm 0.01	3.19% \pm 0.01	3.18% \pm 0.01
			10^{-5}	<u>2.87% \pm 0.01</u>	3.17% \pm 0.01	2.86% \pm 0.01
			10^{-4}	3.26% \pm 0.01	<u>2.99% \pm 0.01</u>	3.21% \pm 0.01
			10^{-3}	2.90% \pm 0.01	3.29% \pm 0.01	5.67% \pm 0.01
			10^{-2}	11.14% \pm 0.03	10.74% \pm 0.03	37.32% \pm 0.00
			10^{-1}	37.32% \pm 0.00	37.32% \pm 0.00	37.32% \pm 0.00
			CPU time (s)	23.844	24.039	24.074
Breast Cancer	Min-max normalization	Hom. quadratic	10^{-7}	3.32% \pm 0.01	3.32% \pm 0.01	3.32% \pm 0.01
			10^{-6}	3.22% \pm 0.01	3.22% \pm 0.01	3.22% \pm 0.01
			10^{-5}	3.36% \pm 0.01	3.36% \pm 0.01	3.36% \pm 0.01
			10^{-4}	3.27% \pm 0.01	3.27% \pm 0.01	3.23% \pm 0.01
			10^{-3}	3.29% \pm 0.01	3.29% \pm 0.01	3.26% \pm 0.01
			10^{-2}	3.24% \pm 0.01	3.24% \pm 0.01	3.16% \pm 0.01
			10^{-1}	<u>3.09% \pm 0.01</u>	<u>3.09% \pm 0.01</u>	2.91% \pm 0.01
			CPU time (s)	40.660	40.554	41.035
Blood Transfusion	Standardization	Inhom. cubic	10^{-7}	21.61% \pm 0.01	<u>21.47% \pm 0.01</u>	21.46% \pm 0.02
			10^{-6}	<u>21.54% \pm 0.02</u>	21.48% \pm 0.02	21.33% \pm 0.02
			10^{-5}	21.63% \pm 0.01	21.63% \pm 0.01	22.09% \pm 0.01
			10^{-4}	23.69% \pm 0.00	23.67% \pm 0.00	23.80% \pm 0.00
			10^{-3}	23.80% \pm 0.00	23.80% \pm 0.00	23.80% \pm 0.00
			10^{-2}	25.38% \pm 0.11	25.38% \pm 0.11	30.94% \pm 0.22
			10^{-1}	47.61% \pm 0.36	47.61% \pm 0.36	52.37% \pm 0.37
			CPU time (s)	52.918	52.915	52.598
Mammographic Mass	Min-max normalization	Hom. cubic	10^{-7}	16.58% \pm 0.02	16.31% \pm 0.02	16.58% \pm 0.02
			10^{-6}	16.46% \pm 0.01	16.15% \pm 0.01	<u>16.46% \pm 0.01</u>
			10^{-5}	16.51% \pm 0.02	16.67% \pm 0.01	16.54% \pm 0.02
			10^{-4}	<u>16.45% \pm 0.02</u>	16.39% \pm 0.01	16.54% \pm 0.01
			10^{-3}	17.34% \pm 0.02	16.84% \pm 0.02	17.86% \pm 0.02
			10^{-2}	18.05% \pm 0.02	18.30% \pm 0.02	18.87% \pm 0.02
			10^{-1}	19.86% \pm 0.01	19.93% \pm 0.01	19.50% \pm 0.01
			CPU time (s)	71.626	71.648	71.730
Qsar Biodegradation	Min-max normalization	Hom. quadratic	10^{-7}	13.85% \pm 0.01	13.85% \pm 0.01	13.84% \pm 0.01
			10^{-6}	13.69% \pm 0.01	13.69% \pm 0.01	13.81% \pm 0.01
			10^{-5}	13.71% \pm 0.01	13.71% \pm 0.01	13.61% \pm 0.01
			10^{-4}	13.86% \pm 0.01	13.86% \pm 0.01	13.70% \pm 0.01
			10^{-3}	<u>13.63% \pm 0.01</u>	<u>13.63% \pm 0.01</u>	15.37% \pm 0.02
			10^{-2}	16.11% \pm 0.01	16.11% \pm 0.01	24.16% \pm 0.02
			10^{-1}	28.27% \pm 0.03	28.27% \pm 0.03	33.78% \pm 0.00
			CPU time (s)	150.642	153.172	150.420

Table B.16: Average out-of-sample testing errors and standard deviations over 96 runs of the robust model. Holdout: 50% training set-50% testing set (continued).

Dataset	Data transformation	Kernel	ρ	Robust		
				$p = 1$	$p = 2$	$p = \infty$
Arrhythmia	-	Inhom. linear	10^{-7}	<u>26.70% ± 0.07</u>	27.47% ± 0.06	28.82% ± 0.06
			10^{-6}	<u>28.00% ± 0.06</u>	<u>27.21% ± 0.06</u>	28.15% ± 0.07
			10^{-5}	28.66% ± 0.06	28.29% ± 0.06	28.10% ± 0.06
			10^{-4}	28.78% ± 0.06	28.04% ± 0.06	<u>27.84% ± 0.07</u>
			10^{-3}	27.41% ± 0.06	28.68% ± 0.07	32.29% ± 0.06
			10^{-2}	31.56% ± 0.07	30.43% ± 0.07	29.41% ± 0.00
			10^{-1}	29.45% ± 0.00	29.45% ± 0.00	29.41% ± 0.00
			CPU time (s)	0.151	0.161	0.142
Parkinson	Min-max normalization	Hom. quadratic	10^{-7}	18.87% ± 0.04	18.00% ± 0.04	17.73% ± 0.04
			10^{-6}	18.37% ± 0.04	17.23% ± 0.04	18.12% ± 0.04
			10^{-5}	18.77% ± 0.04	17.84% ± 0.04	18.15% ± 0.04
			10^{-4}	17.65% ± 0.04	17.18% ± 0.04	17.62% ± 0.04
			10^{-3}	17.43% ± 0.04	17.46% ± 0.04	17.93% ± 0.04
			10^{-2}	<u>16.96% ± 0.04</u>	<u>17.18% ± 0.04</u>	<u>17.07% ± 0.03</u>
			10^{-1}	17.04% ± 0.03	17.22% ± 0.03	24.66% ± 0.00
			CPU time (s)	0.301	0.304	0.303
Heart disease	Min-max normalization	Inhom. linear	10^{-7}	19.99% ± 0.03	20.39% ± 0.03	20.97% ± 0.03
			10^{-6}	20.93% ± 0.03	20.59% ± 0.03	21.17% ± 0.03
			10^{-5}	20.91% ± 0.03	20.88% ± 0.03	20.97% ± 0.03
			10^{-4}	20.51% ± 0.03	20.25% ± 0.03	20.49% ± 0.03
			10^{-3}	20.65% ± 0.03	20.51% ± 0.02	20.31% ± 0.02
			10^{-2}	21.08% ± 0.03	<u>19.64% ± 0.03</u>	19.75% ± 0.02
			10^{-1}	<u>19.98% ± 0.02</u>	19.89% ± 0.02	<u>19.47% ± 0.02</u>
			CPU time (s)	0.643	0.640	0.649
Dermatology	Min-max normalization	Inhom. cubic	10^{-7}	2.45% ± 0.02	2.31% ± 0.02	2.11% ± 0.02
			10^{-6}	<u>2.06% ± 0.02</u>	2.29% ± 0.02	2.19% ± 0.02
			10^{-5}	2.46% ± 0.02	2.32% ± 0.02	<u>2.04% ± 0.01</u>
			10^{-4}	2.46% ± 0.02	<u>2.13% ± 0.01</u>	2.12% ± 0.02
			10^{-3}	2.23% ± 0.02	2.30% ± 0.01	25.62% ± 0.08
			10^{-2}	30.97% ± 0.00	30.97% ± 0.00	30.97% ± 0.00
			10^{-1}	30.97% ± 0.00	30.97% ± 0.00	30.97% ± 0.00
			CPU time (s)	1.015	1.028	1.050
Climate Model Crashes	-	Inhom. linear	10^{-7}	7.15% ± 0.01	7.14% ± 0.01	7.40% ± 0.02
			10^{-6}	7.19% ± 0.01	7.20% ± 0.01	7.11% ± 0.01
			10^{-5}	7.27% ± 0.01	<u>6.98% ± 0.01</u>	7.15% ± 0.01
			10^{-4}	7.27% ± 0.01	7.16% ± 0.01	7.29% ± 0.01
			10^{-3}	<u>7.10% ± 0.01</u>	7.07% ± 0.01	<u>6.98% ± 0.01</u>
			10^{-2}	7.17% ± 0.01	7.12% ± 0.01	7.71% ± 0.01
			10^{-1}	8.50% ± 0.00	8.49% ± 0.00	8.52% ± 0.00
			CPU time (s)	2.776	2.847	2.769

Table B.17: Average out-of-sample testing errors and standard deviations over 96 runs of the robust model. Holdout: 25% training set-75% testing set.

Dataset	Data transformation	Kernel	ρ	Robust		
				$p = 1$	$p = 2$	$p = \infty$
Breast Cancer Diagnostic	Standardization	Inhom. linear	10^{-7}	4.78% \pm 0.01	4.81% \pm 0.01	4.60% \pm 0.01
			10^{-6}	4.84% \pm 0.01	4.74% \pm 0.02	4.94% \pm 0.01
			10^{-5}	4.65% \pm 0.01	4.85% \pm 0.01	4.76% \pm 0.01
			10^{-4}	4.86% \pm 0.01	4.86% \pm 0.01	4.82% \pm 0.01
			10^{-3}	4.89% \pm 0.01	4.76% \pm 0.01	4.79% \pm 0.01
			10^{-2}	4.22% \pm 0.01	4.72% \pm 0.02	<u>3.91% \pm 0.01</u>
			10^{-1}	3.68% \pm 0.01	<u>3.74% \pm 0.01</u>	4.91% \pm 0.01
			CPU time (s)	3.242	3.271	3.231
Breast Cancer	Min-max normalization	Hom. quadratic	10^{-7}	3.81% \pm 0.01	3.73% \pm 0.01	3.59% \pm 0.01
			10^{-6}	3.77% \pm 0.01	3.83% \pm 0.01	3.65% \pm 0.01
			10^{-5}	3.63% \pm 0.01	3.65% \pm 0.01	3.66% \pm 0.01
			10^{-4}	3.57% \pm 0.01	3.69% \pm 0.01	3.53% \pm 0.01
			10^{-3}	3.84% \pm 0.01	3.97% \pm 0.01	3.76% \pm 0.01
			10^{-2}	3.37% \pm 0.01	3.46% \pm 0.01	3.25% \pm 0.01
			10^{-1}	<u>3.18% \pm 0.01</u>	<u>3.15% \pm 0.01</u>	2.90% \pm 0.00
			CPU time (s)	5.301	5362	5.309
Blood Transfusion	Standardization	Hom. cubic	10^{-7}	23.21% \pm 0.01	23.20% \pm 0.02	23.25% \pm 0.01
			10^{-6}	23.41% \pm 0.01	23.28% \pm 0.01	23.34% \pm 0.01
			10^{-5}	23.36% \pm 0.01	23.47% \pm 0.02	23.19% \pm 0.01
			10^{-4}	23.24% \pm 0.01	23.45% \pm 0.01	23.44% \pm 0.01
			10^{-3}	23.08% \pm 0.01	<u>23.15% \pm 0.01</u>	<u>23.12% \pm 0.01</u>
			10^{-2}	23.34% \pm 0.01	23.26% \pm 0.02	23.54% \pm 0.00
			10^{-1}	23.61% \pm 0.00	23.58% \pm 0.00	23.69% \pm 0.00
			CPU time (s)	6.952	6.904	6.936
Mammographic Mass	Min-max normalization	Hom. cubic	10^{-7}	<u>17.62% \pm 0.01</u>	17.83% \pm 0.02	17.84% \pm 0.02
			10^{-6}	17.99% \pm 0.01	<u>17.61% \pm 0.01</u>	17.59% \pm 0.01
			10^{-5}	17.62% \pm 0.02	17.98% \pm 0.01	17.97% \pm 0.02
			10^{-4}	17.69% \pm 0.01	17.62% \pm 0.01	17.79% \pm 0.02
			10^{-3}	17.83% \pm 0.01	18.06% \pm 0.01	18.22% \pm 0.01
			10^{-2}	18.58% \pm 0.01	18.60% \pm 0.01	19.19% \pm 0.01
			10^{-1}	19.82% \pm 0.01	19.79% \pm 0.01	19.64% \pm 0.01
			CPU time (s)	9.039	9.169	9.280
Qsar Biodegradation	Min-max normalization	Hom. quadratic	10^{-7}	15.52% \pm 0.01	15.48% \pm 0.01	15.61% \pm 0.01
			10^{-6}	15.23% \pm 0.01	<u>15.30% \pm 0.01</u>	<u>15.38% \pm 0.01</u>
			10^{-5}	15.28% \pm 0.01	15.31% \pm 0.01	15.47% \pm 0.02
			10^{-4}	15.56% \pm 0.01	15.47% \pm 0.01	15.19% \pm 0.01
			10^{-3}	15.26% \pm 0.01	15.31% \pm 0.01	16.43% \pm 0.02
			10^{-2}	17.60% \pm 0.02	17.64% \pm 0.02	25.20% \pm 0.03
			10^{-1}	28.17% \pm 0.03	28.24% \pm 0.03	33.75% \pm 0.00
			CPU time (s)	18.725	18.756	18.937

Table B.18: Average out-of-sample testing errors and standard deviations over 96 runs of the robust model. Holdout: 25% training set-75% testing set (continued).

Dataset	Data transformation	Kernel	ρ	Robust		
				$p = 1$	$p = 2$	$p = \infty$
Iris	-	Gaussian RBF	10^{-7}	4.00% \pm 0.03	3.86% \pm 0.03	3.43% \pm 0.03
			10^{-6}	3.55% \pm 0.03	3.43% \pm 0.03	<u>2.87% \pm 0.03</u>
			10^{-5}	3.46% \pm 0.03	3.43% \pm 0.03	3.27% \pm 0.03
			10^{-4}	3.15% \pm 0.03	<u>3.21% \pm 0.03</u>	3.01% \pm 0.03
			10^{-3}	<u>3.07% \pm 0.03</u>	3.63% \pm 0.03	3.52% \pm 0.03
			10^{-2}	3.21% \pm 0.03	3.46% \pm 0.03	3.27% \pm 0.03
			10^{-1}	5.83% \pm 0.04	6.31% \pm 0.04	10.87% \pm 0.08
			CPU time (s)	5.684	5.627	5.604
Wine	Standardization	Inhom. linear	10^{-7}	3.48% \pm 0.02	<u>2.63% \pm 0.02</u>	2.89% \pm 0.02
			10^{-6}	2.91% \pm 0.02	3.13% \pm 0.03	3.15% \pm 0.02
			10^{-5}	3.29% \pm 0.02	3.46% \pm 0.03	3.15% \pm 0.03
			10^{-4}	2.79% \pm 0.02	2.63% \pm 0.03	2.89% \pm 0.02
			10^{-3}	2.89% \pm 0.02	2.94% \pm 0.02	2.91% \pm 0.03
			10^{-2}	2.70% \pm 0.02	3.10% \pm 0.02	<u>2.51% \pm 0.02</u>
			10^{-1}	<u>2.63% \pm 0.02</u>	2.65% \pm 0.02	5.71% \pm 0.04
			CPU time (s)	8.361	8.352	8.605

Table B.19: Average out-of-sample testing errors and standard deviations over 96 runs of the robust multiclass model. Holdout: 75% training set-25% testing set.

Dataset	Data transformation	Kernel	ρ	Robust		
				$p = 1$	$p = 2$	$p = \infty$
Iris	Min-max normalization	Gaussian RBF	10^{-7}	4.76% \pm 0.02	4.97% \pm 0.02	4.99% \pm 0.02
			10^{-6}	4.92% \pm 0.02	<u>4.54% \pm 0.02</u>	5.04% \pm 0.02
			10^{-5}	4.78% \pm 0.02	4.63% \pm 0.02	4.92% \pm 0.02
			10^{-4}	4.67% \pm 0.02	5.21% \pm 0.03	4.42% \pm 0.02
			10^{-3}	<u>4.58% \pm 0.02</u>	4.67% \pm 0.02	<u>4.35% \pm 0.02</u>
			10^{-2}	4.69% \pm 0.02	4.63% \pm 0.02	4.90% \pm 0.02
			10^{-1}	6.00% \pm 0.03	6.10% \pm 0.03	15.49% \pm 0.10
			CPU time (s)	1.863	1.870	1.875
Wine	Standardization	Hom. linear	10^{-7}	3.43% \pm 0.02	3.68% \pm 0.02	3.48% \pm 0.02
			10^{-6}	3.51% \pm 0.02	3.73% \pm 0.02	3.41% \pm 0.02
			10^{-5}	3.52% \pm 0.02	3.79% \pm 0.02	3.46% \pm 0.02
			10^{-4}	3.48% \pm 0.02	3.57% \pm 0.02	<u>3.32% \pm 0.02</u>
			10^{-3}	3.69% \pm 0.02	3.79% \pm 0.02	3.45% \pm 0.02
			10^{-2}	3.28% \pm 0.02	3.45% \pm 0.02	3.53% \pm 0.02
			10^{-1}	<u>3.25% \pm 0.02</u>	<u>3.28% \pm 0.02</u>	5.14% \pm 0.03
			CPU time (s)	3.311	3.089	3.148

Table B.20: Average out-of-sample testing errors and standard deviations over 96 runs of the robust multiclass model. Holdout: 50% training set-50% testing set.

Dataset	Data transformation	Kernel	ρ	Robust		
				$p = 1$	$p = 2$	$p = \infty$
Iris	-	Inhom. quadratic	10^{-7}	<u>$4.94\% \pm 0.02$</u>	$5.11\% \pm 0.03$	$5.06\% \pm 0.03$
			10^{-6}	$5.23\% \pm 0.03$	$5.70\% \pm 0.03$	$5.09\% \pm 0.02$
			10^{-5}	$5.22\% \pm 0.03$	<u>$4.97\% \pm 0.03$</u>	$5.06\% \pm 0.02$
			10^{-4}	$5.48\% \pm 0.03$	<u>$5.05\% \pm 0.02$</u>	<u>$4.86\% \pm 0.02$</u>
			10^{-3}	$5.12\% \pm 0.02$	$5.59\% \pm 0.02$	$5.51\% \pm 0.03$
			10^{-2}	$10.37\% \pm 0.07$	$10.70\% \pm 0.07$	$13.22\% \pm 0.08$
			10^{-1}	$26.24\% \pm 0.07$	$25.19\% \pm 0.07$	$31.27\% \pm 0.14$
			CPU time (s)	0.596	0.588	0.593
Wine	Standardization	Gaussian RBF	10^{-7}	$5.21\% \pm 0.07$	$4.06\% \pm 0.03$	$4.56\% \pm 0.06$
			10^{-6}	$4.91\% \pm 0.07$	$3.96\% \pm 0.03$	$4.07\% \pm 0.02$
			10^{-5}	$4.14\% \pm 0.04$	$3.79\% \pm 0.03$	$4.57\% \pm 0.04$
			10^{-4}	$3.45\% \pm 0.02$	$3.71\% \pm 0.02$	$4.18\% \pm 0.02$
			10^{-3}	$6.23\% \pm 0.06$	$5.49\% \pm 0.06$	$6.43\% \pm 0.03$
			10^{-2}	$11.80\% \pm 0.10$	$12.65\% \pm 0.11$	$20.37\% \pm 0.12$
			10^{-1}	<u>$1.34\% \pm 0.05$</u>	<u>$1.24\% \pm 0.05$</u>	<u>$0.00\% \pm 0.00$</u>
			CPU time (s)	0.718	0.717	0.713

Table B.21: Average out-of-sample testing errors and standard deviations over 96 runs of the robust multiclass model. Holdout: 25% training set-75% testing set.

Dataset	75% training set-25% testing set			50% training set-50% testing set			25% training set-75% testing set		
	Deterministic	Best robust	Improvement ratio	Deterministic	Best robust	Improvement ratio	Deterministic	Best robust	Improvement ratio
Arrhythmia	20.47%	19.12%	6.60%	23.59%	23.44%	0.64%	27.31%	26.70%	2.23%
Parkinson	13.19%	12.37%	6.22%	15.10%	13.84%	8.34%	18.49%	16.96%	8.27%
Heart Disease	17.48%	16.36%	6.41%	18.92%	17.29%	8.62%	21.85%	19.47%	10.89%
Dermatology	1.64%	0.55%	66.46%	1.96%	0.51%	73.98%	3.01%	2.04%	32.23%
Climate Model Crashes	5.01%	4.34%	13.37%	5.35%	5.21%	2.62%	7.15%	6.98%	2.38%
Breast Cancer Diagnostic	3.02%	2.39%	20.86%	3.69%	2.86%	22.49%	5.02%	3.68%	26.69%
Breast Cancer	3.17%	2.97%	6.31%	3.31%	2.91%	12.08%	4.47%	2.90%	35.12%
Blood Transfusion	20.72%	20.55%	0.82%	21.86%	21.33%	2.42%	23.32%	23.08%	1.03%
Mammographic Mass	15.71%	15.42%	1.85%	16.49%	16.15%	2.06%	17.68%	17.59%	0.51%
Qsar Biodegradation	12.88%	11.78%	8.54%	13.67%	13.61%	0.44%	15.29%	15.23%	0.39%
Iris (multiclass)	3.10%	2.87%	7.42%	4.47%	4.35%	2.68%	5.05%	4.86%	3.76%
Wine (multiclass)	2.77%	2.51%	9.39%	3.55%	3.25%	8.45%	4.43%	0.00%	100.00%

Table B.22: Improvement ratios of the robust models over the deterministic counterparts for the three holdouts.

Dataset	Data transformation		Mean value of features	CV of features
Arrhythmia	-	Min	2.23×10^2	0
		Max	6.20×10^2	5.29×10^{-1}
Parkinson	Min-max normalization	Min	4.40×10^{-5}	7.71×10^{-2}
		Max	1.97×10^2	1.63×10^0
Heart Disease	Standardization	Min	1.45×10^{-1}	1.35×10^{-1}
		Max	2.47×10^2	2.43×10^0
Dermatology	-	Min	1.06×10^{-1}	3.20×10^{-1}
		Max	3.63×10^1	4.29×10^0
Climate Model Crashes	-	Min	5.00×10^{-1}	5.78×10^{-1}
		Max	5.00×10^{-1}	5.78×10^{-1}
Breast Cancer Diagnostic	Min-max normalization	Min	3.79×10^{-3}	1.12×10^{-1}
		Max	8.81×10^2	1.13×10^0
Breast Cancer	Standardization	Min	1.59×10^0	6.41×10^{-1}
		Max	4.39×10^0	1.09×10^0
Blood Transfusion	Standardization	Min	5.51×10^0	7.11×10^{-1}
		Max	1.38×10^3	1.06×10^0
Mammographic Mass	Standardization	Min	2.78×10^0	1.59×10^{-1}
		Max	5.58×10^1	5.57×10^{-1}
Qsar Biodegradation	Min-max normalization	Min	-1.97×10^{-1}	-1.32×10^2
		Max	3.71×10^1	1.19×10^1

Table B.23: Minimum and maximum values for the mean and the coefficient of variation (CV) computed feature-wise. The data transformation refers to the best choice when classifying the holdout 75%-25% with the deterministic model.